



جمهورية العراق
وزارة التعليم العالي والبحث العلمي
جامعة بابل
كلية الهندسة
قسم الهندسة المدنية

تقييم مقاومة طبقة الأكساء الأسفلتية للتشققات الأنعكاسية

رسالة
مقدمة إلى
قسم الهندسة المدنية
كلية الهندسة - جامعة بابل
وهي جزء من متطلبات نيل شهادة ماجستير علوم في الهندسة المدنية

من قبل:

أحمد عباس جاسم

بإشراف:

الأستاذ حامد محمود حمدو
الأستاذ المساعد علي عبد الأمير علوش

Republic of Iraq
Ministry of Higher Education & Scientific Research
University of Babylon
College of Engineering
Department of Civil Engineering



Evaluation of Reflective Cracking Resistance of HMA Overlays

A THESIS
SUBMITTED TO THE COLLEGE OF ENGINEERING
OF BABYLON UNIVERSITY IN PARTIAL
FULFILLMENT OF THE REQUIREMENT FOR THE
DEGREE OF MASTER OF SCIENCE IN CIVIL
ENGINEERING

By:
Ahmed Abbas Jasim

(B.Sc. in Civil Engineering, 2005)

Supervised By:
Professor Hamed M. Hamdou
Assist Professor Ali A. A. Alwash

(February 2008)

(Soffer 1429)

بِسْمِ اللّٰهِ الرَّحْمٰنِ الرَّحِیْمِ

قُلْ لَوْ كَانَ الْبَحْرُ مَدَادًا لِكَلِمَاتِ رَبِّي لَنَفِدَ

الْبَحْرُ قَبْلَ أَنْ تَنْفَدَ كَلِمَاتُ رَبِّي وَلَوْ جِئْنَا

بِمِثْلِهِ مَدَدًا

صَدَقَ اللّٰهُ الْعَلِيِّ الْعَظِيمِ

الكهف (110)

" أن ليس للإنسان قيمة إلا بقدر ما يخدم الإسلام "

أمامي الشهيد محمد باقر الصدر

*Dedicating To My
Family with All of
My Love and
Respect to Them*

Acknowledgment

First, thanks are to **Allah** His almighty for enabling me to complete this work.

Wish to express my deepest gratitude to my supervisors: **Professor Hamed M. Hamdou** (University of Baghdad) and **Assist Professor Ali Abdul Ameer Alwash** (University of Babylon) for their continued valuable guidance and encouragement during the preparation of this work.

I would like to thank the Staff of Highway Laboratory (College of Engineering in Babylon University), and I would like to thank my friend Ghasak Ebrahim Almothfer and all other friends and colleagues.

Ahmed Abbas Jasim

Certificate Of The Examining Committee

We certify that we have read the entitled "**Evaluation of Reflective Cracking Resistance of HMA Overlays**" and as an Examining Committee, examined the student (**Ahmed Abbas Jasim**) in its content and in what is connected with it, and that in our opinion it is adequate as a thesis for degree of **MASTER OF SCIENCE IN CIVIL ENGINEERING (Transportation Engineering)**.

Signature:

Name: Assist Prof. **Ali A. Hussain Abdul-Amir**
(Member)

Date: 17/2/2008

Signature:

Name: Assist Prof. Dr. **Nahla Y. Ahmed**
(Member)

Date: 18/2/2008

Signature:

Name: Assist Prof. Dr. **Ghalib Muhsen Habeeb**
(Chairman)

Date: 23/2/2008

Signature:

Name: Professor **Hamed M. Hamdou**
(Member and Supervisor)

Date: 15/2/2008

Signature:

Name: Assist Prof. **Ali A. A. Alwash**
(Member and Supervisor)

Date: 16/2/2008

Signature:

Name: Assist. Prof. Dr. **Ammar Y. Ali**
(Head of the Civil Engineering Department)

Date: 24/2/2008

Signature:

Name: Assist. Prof. Dr. **Salah Tawfeek Ali Al-Bazzaz**
(Dean of the College of Engineering)

Date: 1/2/2008

التشققات الأنعكاسية

التشققات الأنعكاسية هي تولد و نمو التشققات من التبليط الخرساني (التبليط الصلب) إلى وعبر الأكساء الأسفلتي لطبقات التبليط (التبليط المرن) نتيجة تولد أجهادات الأحمال و درجة الحرارة. أن تمدد وتقلص التبليط الخرساني والناجمة عن التغيرات في درجة الحرارة هي المساهم الرئيسي في توليد هذا النوع من التشققات.

أن الحركة الأفقية (التمدد والتقلص) للتبليط الخرساني نتيجة التغير في درجة الحرارة اليومية أو الموسمية يولد أجهادات أفقية في أسفل طبقة الأكساء الأسفلتي للتبليط, وعندما تصبح تلك الاجهادات أكبر من الحد الاقصى لتحمل الطبقة سوف تتولد التشققات الأنعكاسية في طبقة الأكساء الأسفلتي للتبليط.

ان الهدف الاساسي من هذه الدراسة هو تصنيع جهاز ملائم لفحص طبقة الأكساء الإسفلتي للتبليط وبعد ذلك يتم استعمال هذا الجهاز لبحث العوامل المرتبطة بظروف الطقس وخواص الخلطة الإسفلتية المؤثرة على مقاومة التشققات الأنعكاسية في طبقة الأكساء الأسفلتي للتبليط. إن تلك العوامل المؤثرة تتضمن: درجة حرارة التبليط, مقدار تمدد وتقلص مفصل التبليط الخرساني, محتوى الاسفلت بالخلطة الإسفلتية, نوع المضافات والتدرج المنخلي للركام.

إن مقاومة الخلطة الإسفلتية ضد التشققات الأنعكاسية تزداد بتقليل مقدار تمدد وتقلص مفصل التبليط الخرساني, زيادة سمك طبقة الاكساء الاسفلتية, زيادة في محتوى الاسفلت بالخلطة, زيادة نسبة الركام الخشن في الخلطة واستعمال الاسمنت البورتلاندي كمادة مالئة للخرسانة الاسفلتية.

ومن خلال نتائج هذه الدراسة فإنه يوصى باستعمال الجهاز المصنع محلياً (فحص طبقة الاكساء الإسفلتي للتبليط) لتقييم مقاومة الخلطة الاسفلتية للتشققات الأنعكاسية (لنموذج لا يتجاوز سمكه 30 ملم).

Abstract

Reflective cracking is the propagation of cracks from rigid pavement into and through the hot mix asphalt (HMA) pavement overlay as a result of load-induced and/or temperature-induced stresses. The contraction and expansion of rigid pavement caused by temperature variations is a primary contributor to reflective cracking initiation.

Horizontal movement of rigid pavement by daily and seasonal temperature variation creates tensile stresses in the bottom of HMA pavement overlay layer. When these stresses become greater than the tensile strength of the HMA pavement overlay, cracks develop in the new HMA pavement overlay.

The main objective of this study is to manufacture a suitable Pavement Overlay Tester (POT) and then investigating the factors related to environmental conditions and asphalt concrete mixtures affecting the resistance to reflective cracking of asphalt concrete overlays. The influencing factors included pavement temperature, joint opening, asphalt cement content, filler type and aggregate gradation.

The resistance to reflective cracking has been determined to be improved at elevated pavement temperature, with less joint opening, with thicker overlays, and for paving mixtures with high asphalt content, coarse gradation, and portland cement as a mineral filler.

The locally manufactured Pavement Overlay Tester (POT Apparatus) is recommended to be used in the evaluation process of paving mixtures resistance to reflective cracking (up to 30mm thickness).

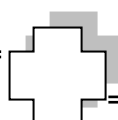
Chapter 1

Introduction

1.1 General

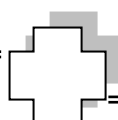
Reflective cracking is defined as the propagation of cracks from the movement of the underlying pavement (flexible or rigid pavement) or base course into and through the new pavement overlay as a result of load-induced and/or temperature-induced stresses. Reflective cracking is considered as one of the most serious problems associated with composite pavements especially when constructed with thin HMA pavement overlays over rigid pavements (**Blankenship et al. 2002**).

The most serious problems are not the cracks appearing in the pavement overlays surface, but the deterioration of the ride quality and serviceability of the pavement overlays, the base layer, and loss of support underneath the rigid pavements. These failure criteria are caused by water and/or moisture infiltration, freeze and thaw cycles, temperature change cycles, and repeated loadings leading to rapid deterioration of the pavement structure and foundation (i.e. Reflective cracking is accelerating the deterioration of the pavement structure) (**Blankenship et al. 2002**).



Cracks appear in the pavement overlays primarily through either fatigue or reflective cracking mechanism. The fatigue test itself has not been implemented as a design tool primarily because the test procedure is very time consuming. It can take several weeks with expensive repeated load test equipment to obtain single fatigue curve. On the other hand, reflective cracking is initiated by existing discrete subsurface defects such as joints, cracks or areas of stripping, and the reflective cracking test procedure is not time consuming, so it has been implemented as a design tool primarily and it could be gets on reflective cracking curve in one day or less (**Zhou and Scullion 2005**).

The cause of reflective cracking can be either traffic or environmental factors. In order to perform well in the field, a pavement overlay must have a balance of both good rut and crack resistance properties. Yet, there is a lack of simple test equipment and rapid procedure for routine use to characterize the reflective cracking resistance of asphalt mixture. Therefore, there is an urgent need to develop a practical test equipment for characterizing the reflective cracking resistance of asphalt mixture (**Zhou and Scullion 2005**).



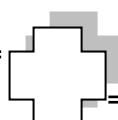
1.2 Research Objective

The objective of this work is to manufacture a suitable Pavement Overlay Tester (POT) based on the principles suggested by Texas Transportation Institute and then investigating the factors related to environmental conditions and asphalt concrete mixtures (using the locally available materials) affecting the resistance to reflective cracking of asphalt concrete overlays.

1.3 Layout of Thesis

To achieve the objective of this research, the work should include the following:

- 1- Chapter two is focused on the review of literature related to reflective cracking phenomenon.
- 2- The details of the experimental work required for this study with the information on material properties and testing equipment are given in chapter three.
- 3- The research results and discussion are presented in chapter four.
- 4- Finally, the extracted conclusions from previous chapters and recommendations for further studies are presented in chapter five.



Chapter 2

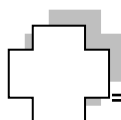
Literature Review

2.1 Introduction

HMA overlays are applied to an existing pavement (flexible or rigid) when the structural or functional conditions of the pavement has reached an unacceptable level of deterioration. Most of the overlays are designed to reflect the increase in pavement resistance to fatigue and rutting distresses (**Bayomy et al. 1996; Pierce et al. 1993**).

The use of HMA pavement overlays presents a long-term and economical solution to the pavement rehabilitation problem. HMA pavement overlays providing restore ride ability, improve the long-term functional pavement performance as well as increase the structural capacity of the existing pavement system. Due to the expense, time and traffic delay involved in rigid pavements restoration and reconstruction, resurfacing of rigid pavements with HMA pavement overlays is a very appealing option for many countries (**Decker and Hansen**).

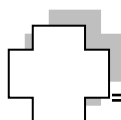
Many HMA overlays prematurely exhibit a cracking pattern similar to that in the old underlying pavement (rigid pavement). The cracking in the new overlay surface is due to the inability of the overlay to withstand shear and tensile stresses created by movements concentrated around preexisting cracks in the underlying pavement (rigid pavement) (**Cleveland et al. 2002**).



The opening and closing of joints (or cracks) of rigid pavement caused by temperature cycles is a primary and a major contributor to reflective cracking initiation and take part in the initial propagation; then, traffic loadings play the role in the second step of the crack propagation. This movement may be due to traffic loading causing differential deflections at cracks (or joints) in the underlying pavement layers, expansion or contraction of subgrade soils, expansion or contraction of pavement itself due to changes in temperature and/or combinations of these phenomena (**Cleveland et al. 2002**).

Pavement movement, induced by any of the above causes, creates shear and/or tensile stresses in the new overlay. When these stresses become greater than the shear or tensile strength of the HMA, a crack develops in the new overlay. This propagation of an existing cracking pattern from the old pavement (rigid pavement) into and through a new overlay is know as a reflective cracking (**Cleveland et al. 2002**).

Reflective cracks through HMA overlays have been an international problem for decades. Although reflection cracks do not generally reduce the structural capacity of a pavement, subsequent ingress of moisture and the effects of the natural environment and traffic can lead to the premature distress and even failure of the pavement. Many different treatments have been tried over the years to prevent reflection cracking; none have been successful. However, some treatments have shown significant delays in the appearance and reductions in the amount and severity of reflective cracks (**Cleveland et al. 2002**).



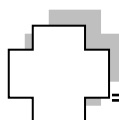
2.2 Types of Reflective Cracking

Reflective cracking is most common in asphalt overlays placed on rigid pavements, but it also occurs in asphalt overlays on cracked asphalt concrete pavements, and in asphalt pavements with stabilized bases. Two types of reflective cracking are shown in Figure (2.1): traditional single reflective cracking and double reflective cracking. When and which type of reflective cracking occurs depends upon the degree of horizontal joint or crack (in the underlying pavement) movement and the magnitude of vertical deflections across the joint or crack (in the underlying pavement) induced by traffic load and environmental effects (Zhou and Scullion 2005).



(a) Traditional Single Reflective Cracking (b) Double Reflective Cracking

Figure (2.1) Types of Reflective Cracking (Zhou and Scullion 2005).

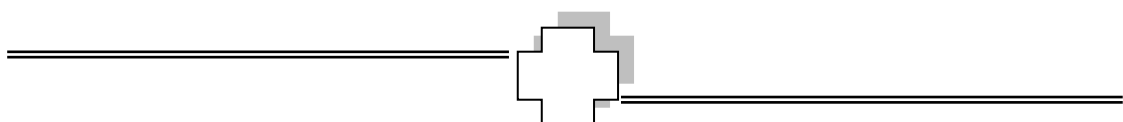


Double reflective cracks reported by **Marchand and Goacolou (1982)**, **Gaarkeuken et al. (1996)**, and **Zhou and Sun (2002)** are located a few inches on each side of the centerline of the old joint (or crack). Compared to the traditional single reflective cracking located directly above the joint (or crack), and double reflective cracking is less frequent than the traditional single reflective crack case.

Advanced three-dimensional finite element analysis results (**Zhou and Sun 2002**) indicate that the double reflective cracking occurred only at joints (or cracks) with significant vertical movement, such as thin asphalt overlays over existing Portland cement concrete (PCC) pavements with poor support.

Therefore, generally the HMA pavement overlay has traditional single reflective cracking, so in this study the traditional single reflective cracking phenomenon will be discussed because it is more frequent.

Traditional single reflective cracking means that only one crack is observed at the surface of the asphalt overlay directly above the joint or crack in the existing pavement (rigid pavement). This type of reflective cracking is caused mainly by the daily temperature variations, especially in the winter time. Daily temperature variations are the primary factors inducing horizontal movement of the subsurface joint or crack (in the rigid pavement). If the overlay is fully bounded with the underlying pavement, tensile stress is created in the overlay directly above the joint or crack. This induced tensile stress (i.e. horizontal movement of the rigid pavement) is proportional to the relaxation

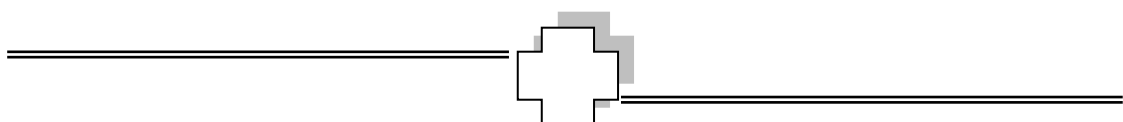


property of the asphalt mixture and the movement taking place in the joint or crack; that, in turn, is proportional to the slab length (or space between the cracks), temperature variation, and the coefficient of thermal expansion (COTE) of the underlying pavement material. When the induced tensile stress exceeds the tensile strength of the asphalt overlay, a single crack directly on top of the joint or crack will occur. With repeated traffic loading and/or temperature variation cycles, the initiated crack will further propagate until reaching the surface of the asphalt overlay (**Zhou and Scullion 2005**).

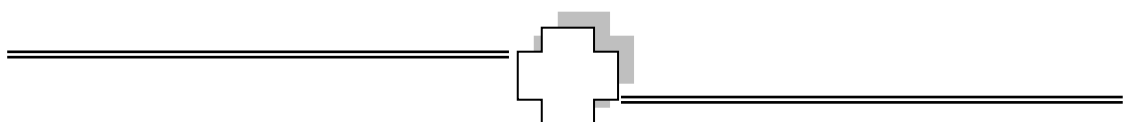
2.3 Mechanisms of Reflective Cracking

Simultaneous movements of an overlay caused by wheel loads, temperatures changes, temperature gradients, and subgrade moisture changes include a complex stress state of cyclic bending, tension, and shear within the overlay. These stresses are caused by a complex sequence of cyclic crack/joint movements caused by vertical and horizontal loads, long-term (seasonal) and short-term (daily) temperature changes and subgrade volume changes due to moisture variations (**Cleveland et al. 2002**).

Lytton (1989) pointed out that, every time a load passes over a crack (or joint) in the old pavement, three pulses of high stress concentrations occur at the tip of the crack, as it grows upward through the overlay are shown in Figure (2.2). The first stress pulse is a maximum shear stress pulse (shown in point A in Figure (2.2)). The



second stress pulse is a maximum bending stress pulse (shown in point B in Figure (2.2)). The third stress pulse is again a maximum shear stress pulse, except that it is in the opposite direction of the first shear pulse. Also, because there is often a void beneath the old surface, the maximum shearing stress when the load is at point C is usually larger than when it is at point A (shown at point C in Figure (2.2)). These stress pulses occur in a very short period of time, in the order of 0.05 second. At these high loading rates, the stiffness of the asphalt concrete in the overlay and in the old pavement is quite high. Each pavement movement results in a small increase in crack length in the overlay. As the number of loadings increases, the magnitude of movement increases, crack growth rate increases, and overlay reflection cracks rapidly appear at the pavement surface .



Position of Wheel Load

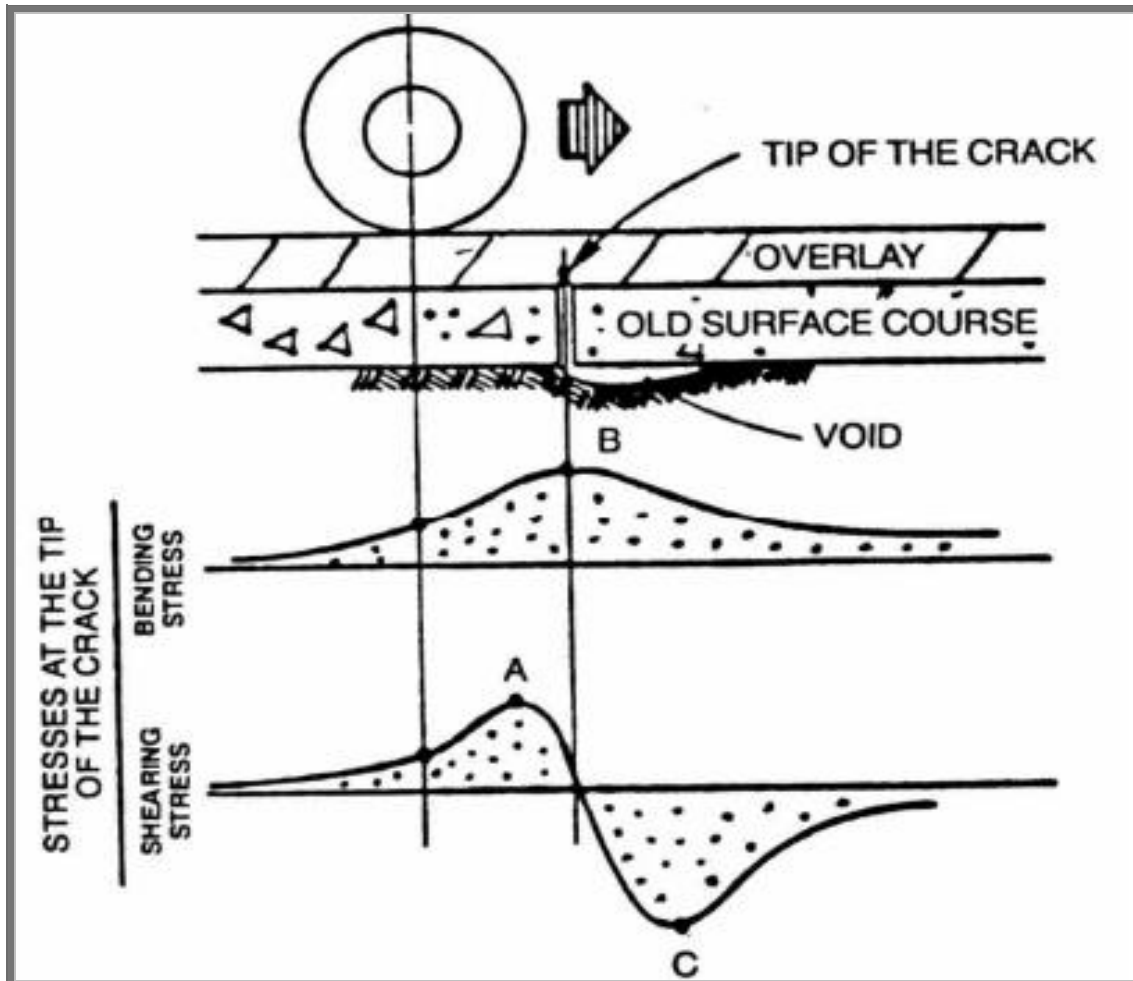
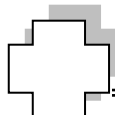


Figure (2.2) Shear and Bending Stress Induced at a Crack Caused With a Moving Wheel Load (Lytton 1989).

More recently, **Read (2000)** acknowledged the merits of fracture mechanics approach to simulate crack propagation in HMA. However, Read emphasized that HMA is a three phase bituminous material (binder matrix, coarse aggregate, and air voids), which differs from continuous (homogeneous) material for which the fracture mechanics theory was developed.



Based on extensive laboratory testing and image analysis technique, **Read (2000)** found that cracks in HMA attempt to follow the shortest route around the interface between the coarse aggregate and the matrix, which appears to be the path of least resistance. If an aggregate is encountered in this path, the crack propagation would be delayed. In contrast, a void may accelerate this process.

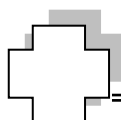
2.4 Fracture Mechanics Approach

The science of fracture mechanics, first publicized in the 1920s by **Griffith**, sets out to describe the propagation of cracks through materials and therefore has relevance to forms of cracking encountered in asphalt pavements (**Sulaiman and Stock 1995**).

Fracture mechanics is an engineering discipline that is primarily drawn up by the disciplines of applied mechanics and materials science. In the most basic form it can be applied to relate the maximum permissible applied load acting upon a structural component to the size and location of crack in the component. It can be used to provide the rate at which a crack can approach a critical size in fatigue or by environment (**Kanninen and Popelar 1985**).

Fracture mechanics deals with the following states of stress:

- a. Plane stress conditions, in which one of the principal stresses is zero. This situation is commonly encountered in the loading of very thin sheets, which do not develop any stress through their thickness.

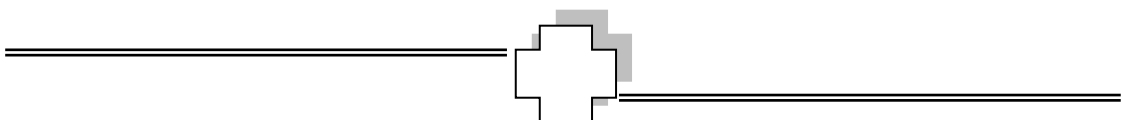


b. Plane strain condition, in which one of the principal strains is zero. A typical example occurs in the central region of a wide strip, which is rolled; here the strip extends as its thickness is reduced, but its width remains virtually constant (**Knott 1976**).

2.4.1 Fracture in the Asphalt Binder

Since **Majidzadeh (1970)** introduced fracture mechanics concepts into the field of pavements, the fracture mechanics approach has been widely used in predicting pavement cracking (fatigue, low temperature, and reflective) analysis. Different from continuum mechanics, the fracture mechanics approach focuses on crack propagation. The occurrence of reflective cracking is a crack propagation process caused by a combination of the three modes of loading are shown in Figure (2.3):

1. **Mode I** loading (opening mode, K_I) results from loads that are applied normally to the crack plane (thermal and traffic loading).
2. **Mode II** loading (sliding mode, K_{II}) results from in-plane shear loading, which leads to crack faces sliding against each other normal to the leading edge of the crack (traffic loading).
3. **Mode III** loading (tearing mode, K_{III}) results from out-of-plane shear loading, which causes sliding of the crack faces parallel to the crack leading edge. Although this mode may occur if the crack plane is not normal to the direction of traffic, this mode of loading is neglected in the more study for simplicity. Compared to Modes I and II, Mode III is rare and is often neglected for simplicity. The fact that the



mechanisms of reflective cracking (bending, shear, and thermal) can be exactly modeled by fracture Modes I and II makes the fracture mechanics approach the best option for modeling reflective cracking.

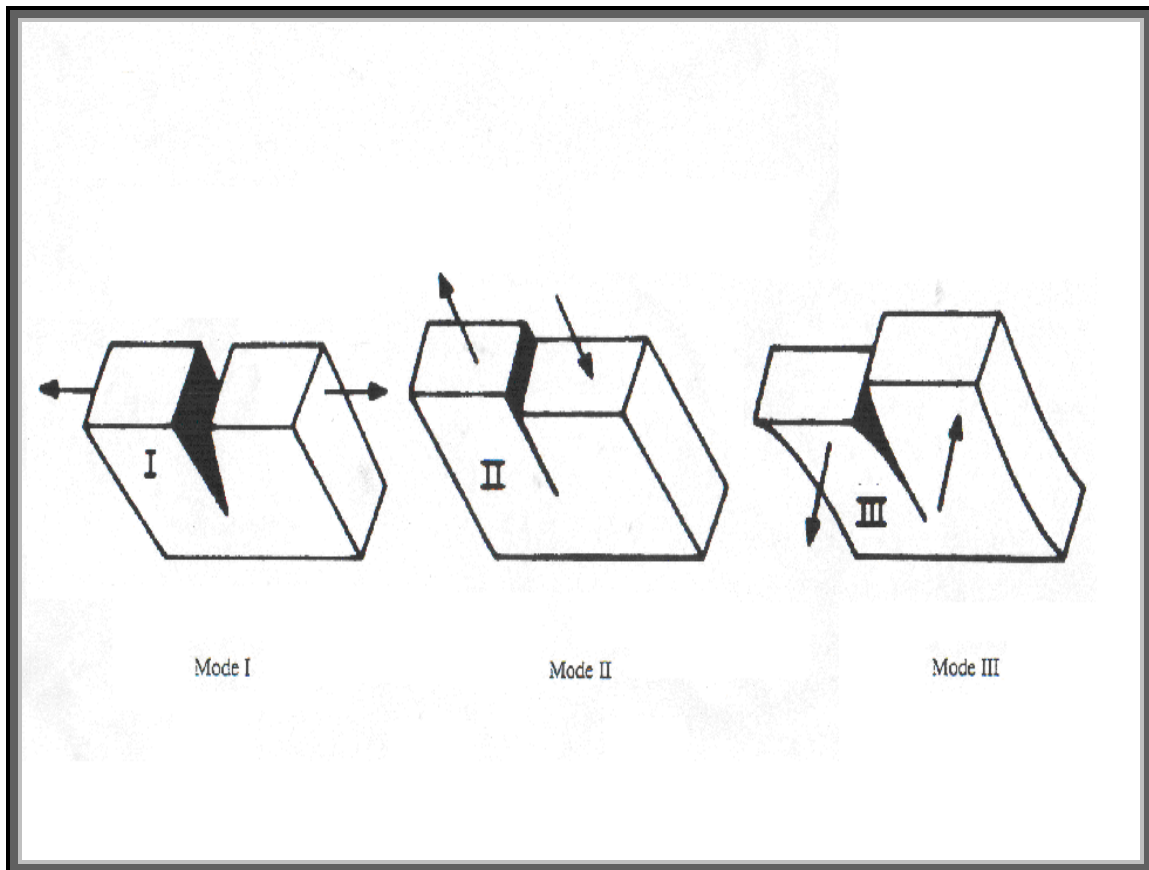
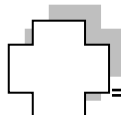


Figure (2.3) The Three Modes of Loading to Describe Crack Growth (Majidzadeh 1970).

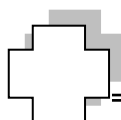
When the pavement surface cools, the asphalt binder will slowly transform from a ductile into a brittle material. Inherent in the pavement structure is a large number of flaws that are unable to transmit loads and will therefore act as stress concentrators. At crack tips in the binder and, at the binder-aggregate interface or within broken



aggregate, thermal induced stresses will concentrate which may allow cracks to initiate and/or propagate (**Ahmed 2003**).

Whether or not crack will propagate under a given thermal shrinkage stress which depends on a balance of energies to form and deform the new fracture surfaces. If the released strain energy exceeds the energy required to form the new crack surfaces, the crack will propagate and failure will result until the crack front is stopped by an insurmountable barrier such as a large aggregate particle (**Lee et al. 1995**).

To establish if the discontinuous crack growth in HMA may be treated using fracture mechanics principles, **Jacobs et al. (1996)** compared the experimental crack growth of HMA (discontinuous crack growth) to the continuous crack growth process as simulated using the finite element method. It was found that although the level of agreement is highly influenced by the mix nominal aggregate size (better agreement was found for mixes with a small aggregate size); the crack growth process in HMA may be accurately described using the fracture mechanics theory.



2.4.2 Stages of Reflective Cracking

Two distinct phases are considered in the cracking process of new pavement systems:

1. The crack initiation phase: which is composed of two stages of microcracking and formation of macrocracks, is defined by the number of load repetitions required to form a visible damaged zone at the bottom of the overlay (**Uzan 1997**). The original damage may occur at the bottom of the HMA layer and grow upwards or it may also directly show at the surface due to the stress concentration around the tire treads (or joint of rigid pavement). The number of cycles of a specific load (by traffic and/or environmental effect) a pavement can withstand before it cracks may be related to the critical strain using a fatigue law (**Vanelstraete et al. 2000**):

$$N_i = C \varepsilon^a \quad \dots\dots\dots (2.1)$$

Where:

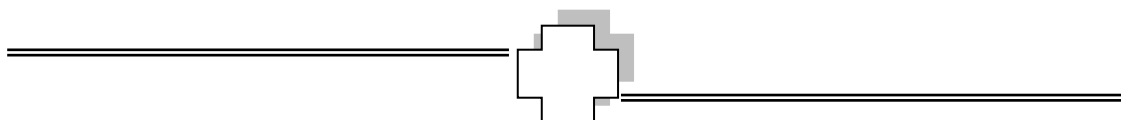
N_i : Number of cycles before crack initiation.

ε : Critical strain.

C : Constant of the fatigue line.

a : Slope of the fatigue curve.

The direction of the strain to be used on Equation (2.1) depends on the failure mechanism under consideration. For example in the case of fatigue cracking, the horizontal tensile strain at the bottom of the



HMA layer is used. In case of reflective cracking induced by Mode II loading, the number of cycles for crack initiation may be determined as follows (**Belgian Road Research Center, BRCC 1998**):

$$N_i = 4.856 \times 10^{-14} \varepsilon_{zx}^{-4.76} \dots\dots\dots (2.2)$$

Where:

N_i : Number of cycles before crack initiation.

ε_{zx} : Shear strains 10 mm above the existing crack.

When the reflection of cracks is considered, the pavement service life against crack initiation may be much shorter than with regular distresses (such as fatigue cracking) since the crack is already well established in the existing pavement.

2. The crack propagation phase: which represents the stage where the crack propagates to the surface through the entire thickness of the HMA overlay. A description of the crack propagation phase in flexible pavements can be based on the empirical power law developed by **Paris and Erdogan (1963)**:

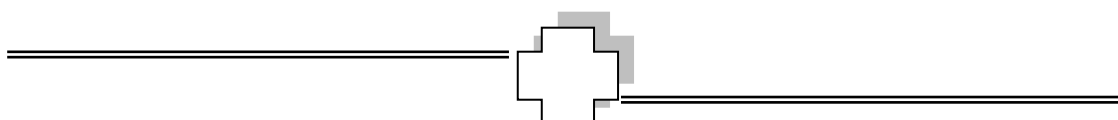
$$\frac{dN}{dc} = A (K)^n \dots\dots\dots (2.3)$$

Where:

c : Crack length.

N : Number of loading cycles.

A and n : Fracture parameters of the material.



K : Stress intensity factor depending on the geometry of the pavement structure, fracture mode , and crack length.

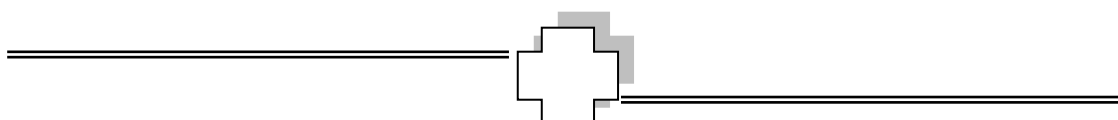
The number of load cycles (N_f) needed to propagate a crack through the asphalt overlay thickness (h) can be estimated by numerical integration in the form of Equation (2.3):

$$N_f = \int_0^h \frac{dc}{A (\Delta K)^n} \dots\dots\dots (2.4)$$

2.4.3 Fracture Parameters of the Material (A and n)

Although the general trend within the pavement society is to believe that Paris' law adequately describes the rate of crack growth in HMA overlay (**Majidzadeh et al. 1969; Lytton 1989**), the application of this approach in this study is valid when acknowledging the following assumptions:

1. Since no exact definition of the stress intensity factor for a multi-layer pavement system is available, a regression analysis was performed to define the stress intensity factor as a function of the crack length (c) for each of the considered designs. The developed regression models are dependent on the assumed stiffness for the pavement layers and the crack propagation resistance of the mix.
2. The computed number of cycles is highly sensitive to the assumed values of the fracture parameters (A and n). The correct way to determine the fracture parameters of a material (A and n) is to examine



the stable crack growth of HMA beam samples under repeated loading conditions, which is a tedious and expensive operation (**Francken 1993**). Since no direct measurements of the fracture parameters (A and n) were feasible in this study, and since such testing are not expected to be conducted in a routine overlay design, theoretical relations between the fracture parameters of the material and its creep properties are suggested (**Schapery 1982**):

$$n = \frac{2}{m} \dots\dots\dots (2.5)$$

Where:

m : Slope of the log creep compliance versus log time curve.

Several relations were proposed to calculate the second fracture parameters (A). For example, model relates the A parameter to the mix properties follows (**Lytton et al. 1993**):

$$\text{Log}A = -2.605104 + 0.184408AV - 4.704209\text{log}AC - 0.00000066E \dots\dots\dots (2.6)$$

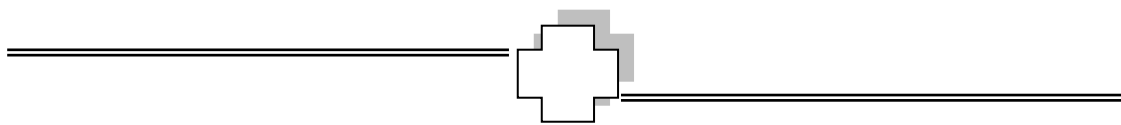
Where:

AV : Air voids (%).

AC : Asphalt content (%).

E : Resilient modulus of the mixture (in psi).

The equation (2.6) was derived based on the results of controlled strain beam fatigue data with a coefficient of determination (R^2) of 0.89. From the previous equation, it can be noticed that the more air



voids or the less asphalt content in the mix, the greater the A parameter, and therefore the shorter the fatigue life. This may explain why stone-mastic asphalt (SMA) provides superior performance than regular mixtures. Stone-mastic asphalt is usually characterized by its high asphalt content, and the lower percentage of air voids.

2.4.4 Stress Intensity Factor (K)

Stress intensity factor (K) is used in the fracture mechanics to specify the stress intensity at crack tip. The stress near crack tip is substantially greater than the nominal stress (**Kanninen and Popelar 1985**).

Irwin developed the stress intensity approach in 1950. He showed that the stress in the vicinity of crack tip take the following form:

$$\sigma_{ij} = \frac{\sigma\sqrt{\pi c}}{\sqrt{2\pi r}} f_{ij}(\theta) \dots\dots\dots (2.7)$$

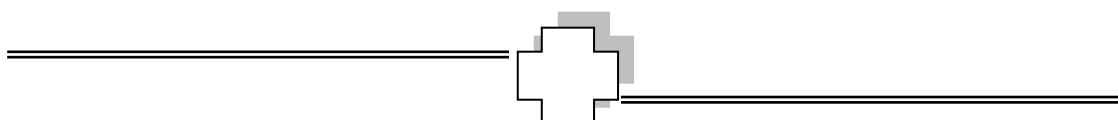
Where:

σ : Nominal stress.

c: Crack length.

r: Distance from the crack tip to the analyzed element.

The stress near crack tip is a function of the $(1/\sqrt{2\pi r})f_{ij}(\theta)$ (geometric position) and a factor $\sigma\sqrt{\pi c}$, which is a simple function of remote stress and crack length. This factor is called "Stress Intensity Factors", K, which gives the elastic stress field. **Griffith's (1920)** analysis



indicates that this characteristic length is the crack length; this turns out that the general form of the stress intensity factor (in unit stress per square root of unit length) is given by:

$$K = \sigma \sqrt{\pi r} f(c/d) \dots\dots\dots (2.8)$$

Where $f(c/d)$ is a dimensionless parameter that depends on the geometry of the component, the length (c) and the crack depth (d). **Ramsamooj (1973), Brooker et al. (1987) and Molenaar (1989)** used finite element model to examine the stress intensity at the crack tip.

2.4.5 Fracture Toughness

Hertzberg (1996) stated that engineers are mostly worried about the brittle fracture because the brittle fracture bring most devastating accidents and happen rapidly and usually the brittle fractures take place when the applied stress reaches the crack tip. The fracture toughness in tension can be defined in terms of the stress intensity factor as:

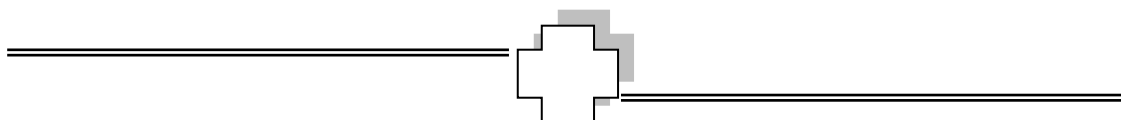
$$K_{IC} = \sigma_f y \sqrt{\pi c} \dots\dots\dots (2.9)$$

Where:

σ_f : The failure stress within the body far away from the crack.

c : The crack length.

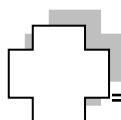
y: Dimensionless parameter that depends on both specimen and crack geometry (y factor usually is 1.0 for the plate of infinite width and 1.1 for the plate of semi-infinite width).



Fracture toughness is a critical value of the stress intensity factor, K_{IC} , at the crack tip necessary to produce failure under simple uniaxial loading (**Shackelford 1992**). If a material does not deform plastically at the crack tip, it is considered brittle and will have low fracture toughness. Conversely, high fracture toughness is usually associated with low strength and/or ductile materials. Therefore, HMA paving materials transition the range of brittle and ductile behavior and the use of Paris' Law, based on linear elastic fracture mechanics, and should be modified to account for the complex nature of this material (**Cleveland et al. 2002**).

2.4.6 Fracture Toughness of Asphalt

Asphaltic concrete mixtures can be characterized as having elastic, viscoelastic, plastic, fracture, and healing material properties (**Lytton et al. 1993**), and **Puzinauskas (1980)** define the asphalt as a macromolecular organic material which is of low viscosity Newtonian liquid at high temperature, a viscous material exhibiting shear-dependent viscoelastic behavior at ambient temperature and a brittle solid at low temperature. Therefore, **Kim and El Hussein (1995)** assumed that the asphalt concrete behaves as an elastic body at low temperature. However since there is no standard method that has been developed for fracture analysis of asphalt materials, many researches (**Anderson et al. 2000**, **Champion-Lapalu et al. 2000**) reported the equation for the critical stress intensity factor (fracture toughness K_{IC}) under a three-points bending beam test



conditions. **Anderson et al. (2000)** present the following equation for K_{IC} calculation.

$$K_{IC} = \frac{P_f S}{BW^{1.5}} \times \frac{3\left(\frac{c}{W}\right)^{0.5} \times \left(1.99 - \frac{c}{W} \left(1 - \frac{c}{W}\right) \times \left(2.15 - 3.93 \frac{c}{W} + 2.7 \frac{c^2}{W^2}\right)\right)}{2\left(1 + 2\frac{c}{W}\right)\left(1 - \frac{c}{W}\right)^{1.5}} \dots(2.10)$$

Where:

P_f : The failure load.

s : The span fixed at 100 mm.

B : The depth of the beam (12.5 mm).

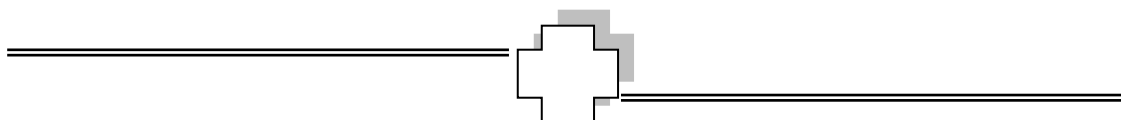
W : The width of the beam (25 mm).

c : The crack length (measured for each test specimen).

Kim and El Hussein (1995) show in their study the change of asphalt concrete fracture toughness by temperature which that fracture toughness increases with the increase in temperature up to a certain point, then decreases.

2.5 Methods of Reducing Reflective Cracking

Many studies have been performed on the subject of reducing or delaying reflective cracking in HMA overlays. **Roberts et al. (1996)** categorized four methods that are commonly employed in the field to reduce reflective cracking:



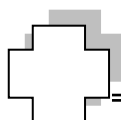
2.5.1 Increasing the HMA Overlay Thickness

Increasing the thickness of HMA overlays to minimize reflective cracking has been based primarily on empirical relations developed from local experience (**Finn and Monismith 1984**). The parameters affecting the thickness of the overlay depend on the type of pavement (HMA or PCC), type of distresses, climatic conditions, and traffic loadings (**Sherman 1982**). **Barksdale (1991)** provides the following HMA overlay thickness information.

- a) Portland cement concrete (PCC) pavements evaluated in Georgia (**Gulden and Brown 1985**) indicated 20 percent area cracking in six years for a 6-inch overlay compared to two years for a 4-inch overlay. Reflective cracking appeared almost immediately after construction for a 2-inch overlay.
- b) Research conducted by **Predoehl (1989)** in California showed that 4.8 inches of overlay is required to reduce reflective cracking for 10 years.

2.5.2 Performing Special Treatments on the Existing Surface

Researchers have investigated the effectiveness of performing special treatments on the existing surface as alternate techniques of minimizing reflective cracking. These treatments have included breaking and seating (or rubblization) of the concrete surface, heater scarification (or pulverization) of the asphaltic surface, and the

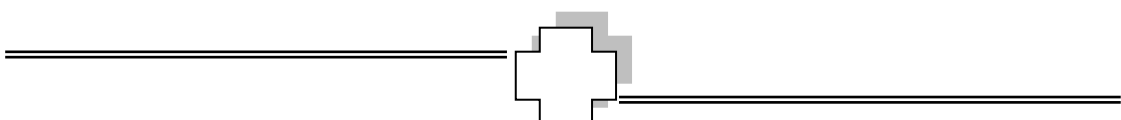


construction of a stress-absorbing membrane interlayer (SAMI) (**Cleveland et al. 2002**).

Generally, the process of breaking and seating or rubblization of the concrete surface involves breaking the existing PCC pavement into small fragments using an impact hammer followed by seating using a vibratory steel-wheel and/or pneumatic roller prior to overlaying. Compaction consolidates the PCC fragments and removes voids or cavities from beneath the PCC pavement and provides a firm support for the pavement structure (**Mclaughlin 1979**).

Pulverization or heater scarification of the HMA surface processes generally involve heater scarification of the existing HMA surface to a specified depth (typically 1 inch) and adding a rejuvenating agent. The mixture is compacted, and a conventional wearing course is normally placed over the recycled pavement. Because this method is limited to surface rehabilitation, the pavement system must be structurally sound (**Button et al. 1994**) to ensure success (**Cleveland et al. 2002**).

The construction of a SAMI normally consists of an asphalt rubber seal coat (**Roberts et al. 1996**). The SAMI is constructed between the existing pavement and the HMA overlay. A typical SAMI consists of 0.6 to 0.8 gal/yd² asphalt rubber material along with just enough aggregate (ranging in size from chips to pea gravel or coarse sand) to provide a working platform (**Sherman 1982**). The thickness of the SAMI ranges from 0.35 to 0.50 inch. The principal objective of the SAMI is the reduction of stresses developed at the crack tip primarily



through the properties of the asphalt rubber material. Results were obtained in investigations summarized by **Barksdale (1991)** where a SAMI was found to delay serious reflective cracking for three to five years. A negative attribute was found from research conducted by **Predoehl (1989)** in California, which indicated that HMA overlays using asphalt rubber SAMIs exhibited bleeding and rutting more frequently than with the use of fabrics.

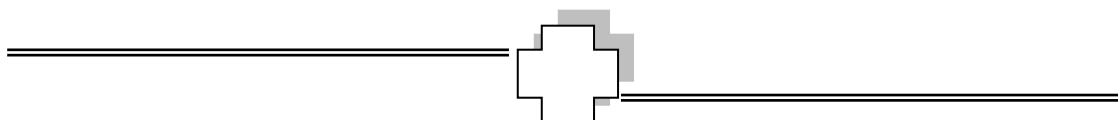
2.5.3 Treatments of Cracks and/or Joints

Treatments only on the cracks and/or joints, as a method of minimizing reflective cracking in HMA overlays, have included cleaning followed by filling the crack or joint with a compressible material, and then applying a narrow strip of bond breaking material (**Cleveland et al. 2002**).

Gurjar et al. (1997) provide guidance on the selection, testing, and performance of joint sealants used in Portland cement concrete (PCC) pavements.

2.5.4 Special Considerations for HMA Overlay Design

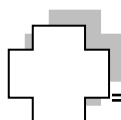
The latest techniques investigated by researchers for reducing reflective cracking have been the use of more compliant asphalts produced by polymer or rubber modification, modification of the bituminous mixture by the addition of synthetic fibers (polypropylene or polyester), the use of ground scrap tire rubber, and installations of



geosynthetic materials such as grids, fabrics, and composites **(Cleveland et al. 2002)**.

The above techniques result in either an increase in the overlay's tensile strength or an increase in its flexibility (compliance). Both of these attributes are important for minimizing reflective cracking, but a balance must be achieved in the mixture design. The use of compliant asphalts, for instance, will improve flexibility but will adversely affect mixture stability, and the pavement will be susceptible to rutting and/or flushing. Conversely, the use of harder asphalts will increase the mixture tensile strength, but flexibility will suffer and the overlay will be susceptible to cracking **(Cleveland et al. 2002)**.

In 1966, a crumb rubber HMA overlay at the Phoenix International Airport performed excellently **(McLaughlin 1979)**. Other pavements constructed in Arizona utilizing rubber modification have resisted fatigue cracking and reduced reflective cracking (McLaughlin 1979). Laboratory and field tests were performed on eight types of chopped synthetic fibers as additives to reduce reflective cracking in HMA overlays ⁽³³⁾. Results from this investigation indicated that fibers added flexibility and improved resistance to crack propagation but increased field compaction requirements **(Cleveland et al. 2002)**.

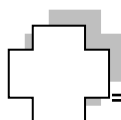


2.6 Factors Influencing Reflective Cracking

Temperature-induced thermal stresses are known to be one of the primary causes of reflection cracking in the asphalt cement concrete (ACC) overlays. Thermal stresses caused by temperature can be separated into three components as shown in Figure (2.4) (**Choubane and Mang 1992**):

- a. Axial displacement is caused by horizontal movement of the pavement surface owing to the temperature gradient.
- b. The bending stress of pavement is induced by the vertical linear temperature differential.
- c. A nonlinear component, generated by the remaining component of temperature, is determined by subtracting the uniform and linear temperature from the total temperature differential.

Most studies for estimating thermal stress considered only horizontal movement components for one-layer systems. Therefore, to model the response of the multilayer pavement systems, additional parameters characterizing pavement structures should be introduced to evaluate thermal stresses in the pavement under field conditions (**McCullough 1998**).



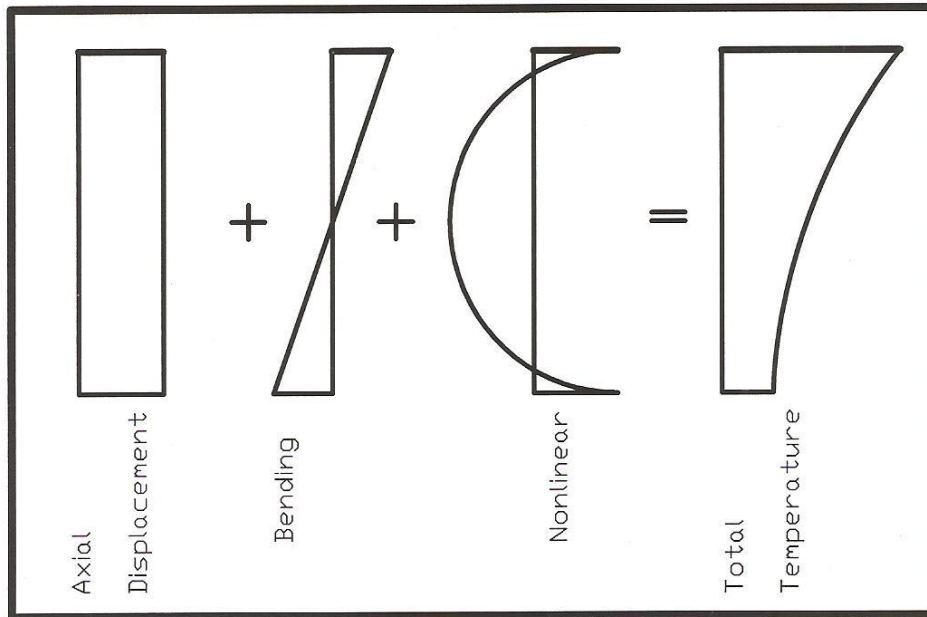
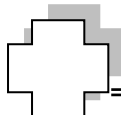


Figure (2.4) Three Components of Temperature Distribution to Thermal Stress in the Pavement (McCullough 1998).

2.6.1 Temperature Distribution in the ACC and PCC Layer

Temperature distributions shown in Figure (2.5) are based on weather information for December in 1993, the maximum surface (ACC Layer) temperature varied from 6.1°C (43°F) to 20°C (68°F), while the temperature in PCC layer ranged between 10°C (50°F) and 15.6°C (60°F). The temperature in the soil layer did not vary as much as did the temperature in the two upper layers. Unlike the ACC Layer, the temperature variation in the PCC layer does not much fluctuate. Figure (2.6) shows variation of the temperature at surface of ACC Layer with the time (McCullough 1998).



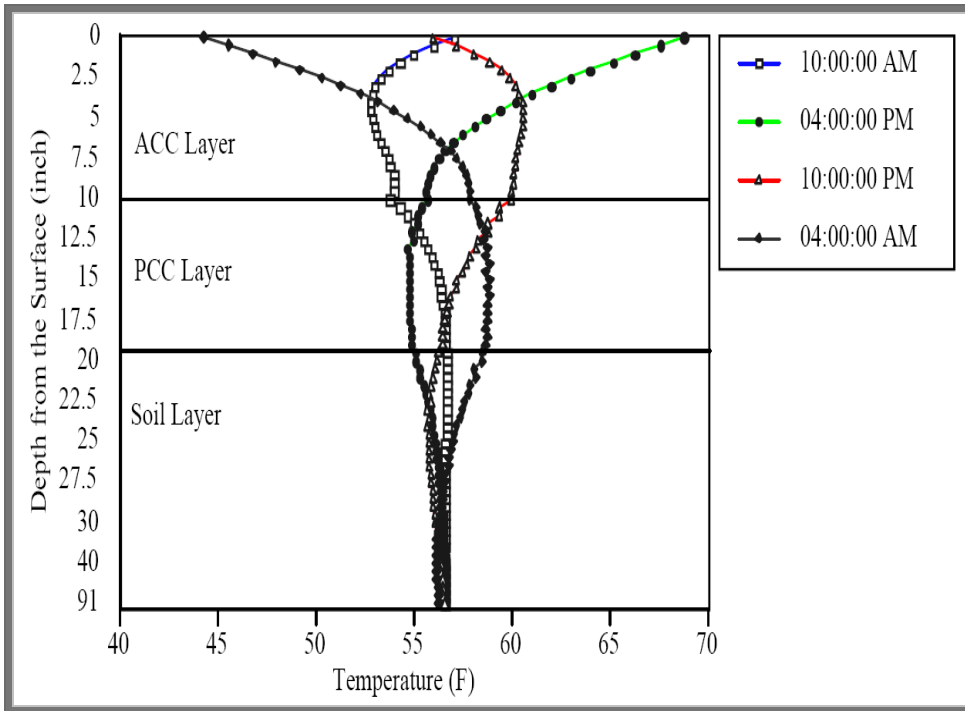


Figure (2.5) Generated Temperature Distribution With Depth in Pavement Structure in Winter (McCullough 1998).

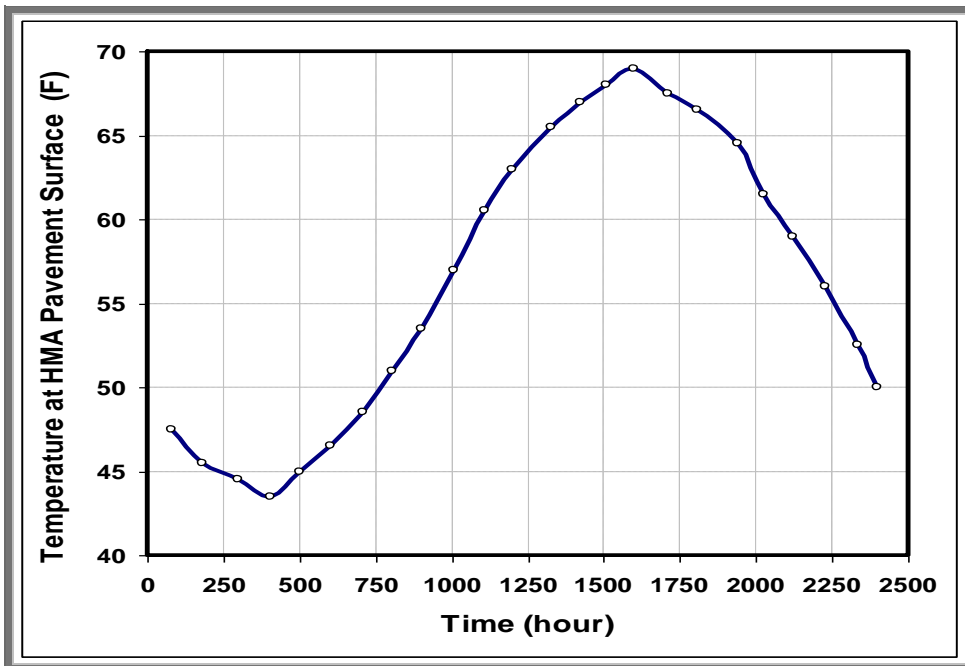
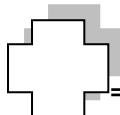


Figure (2.6) Variation of the Temperature at HMA Pavement Overlay Surface and Time in Winter (McCullough 1998).



2.6.2 Effect of Maximum Temperature Difference

Maximum temperature differentials were varied to observe the temperature effect on the pavement response. The inputs were set at 16.7°C (62°F)/day, 28°C (82°F)/day and 39°C (102°F)/day. The maximum daily temperature differential reported from the test section was 16.7°C (62°F)/day. As the maximum temperature differentials increase, the radius of the curvature decreases and maximum deflection increases up to 0.5mm, as shown in Figure (2.7). The temperature effect shown in Figure (2.8) and Figure (2.9) indicates that the horizontal stress (of rigid pavement or HMA pavement overlay) increases when increasing the maximum temperature differentials (McCullough 1998).

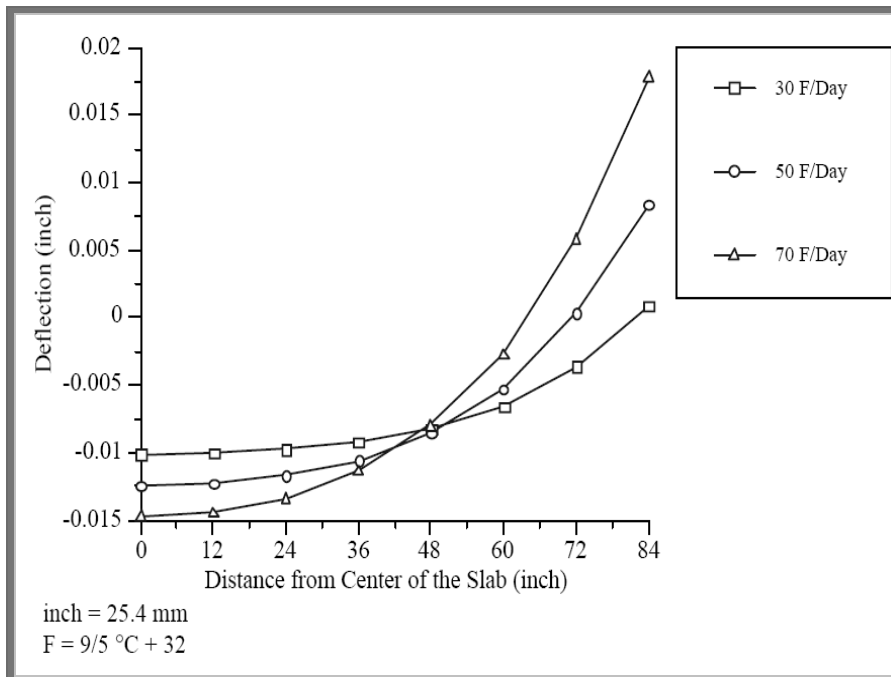
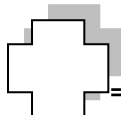


Figure (2.7) Deflection Variation With Different Temperature Differentials (McCullough 1998).



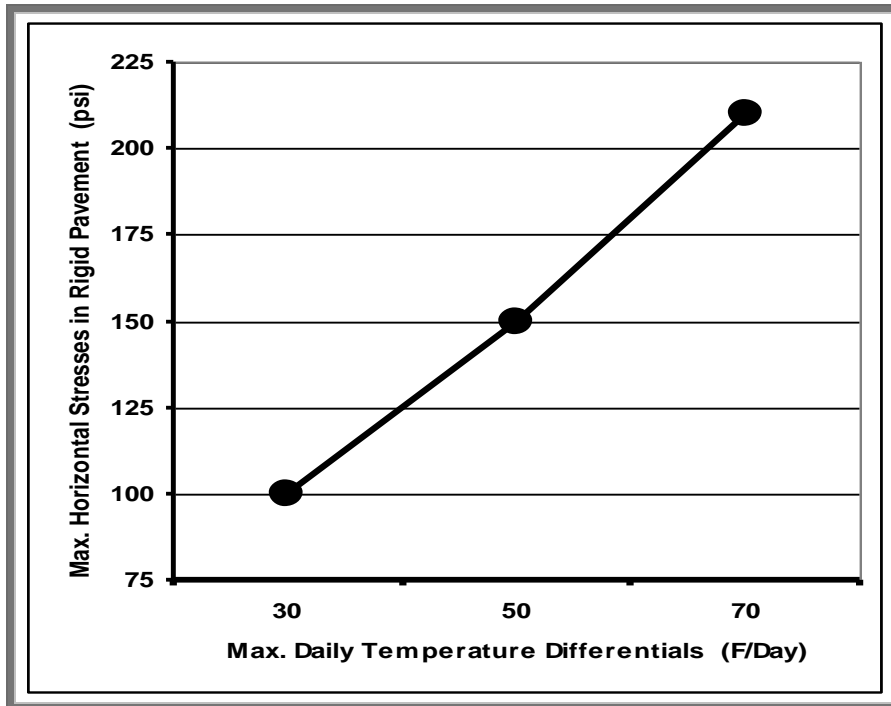


Figure (2.8) Max. Horizontal Stress of Rigid Pavement Variation With Max. Temperature Differentials (McCullough 1998).

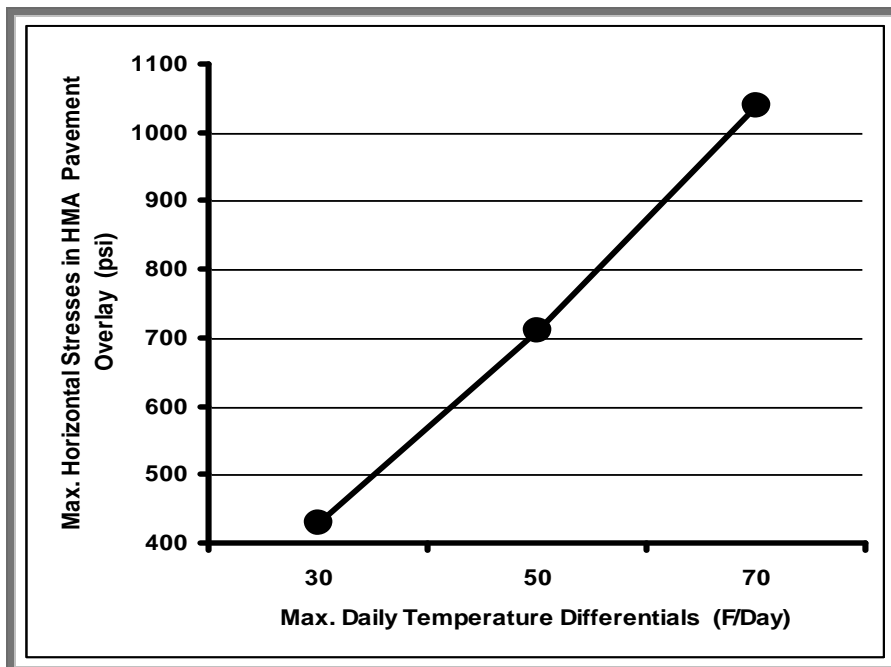
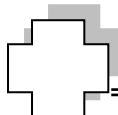


Figure (2.9) Max. Horizontal Stress of HMA Pavement Overlay Variation With Max. Temperature Differentials (McCullough 1998).



2.6.3 Effect of Stiffness and Thickness of HMA Pavement Overlay

The stress variation of each layer due to stiffness variation in the HMA pavement overlay is shown in Figure (2.10) and Figure (2.11). The stress in the rigid pavement does not vary much, but the stress in the HMA pavement overlay increases significantly as stiffness differentials increase. This means that the effect of the stiffness of the HMA pavement overlay is critical for determining whether reflective cracking will occur or not (McCullough 1998).

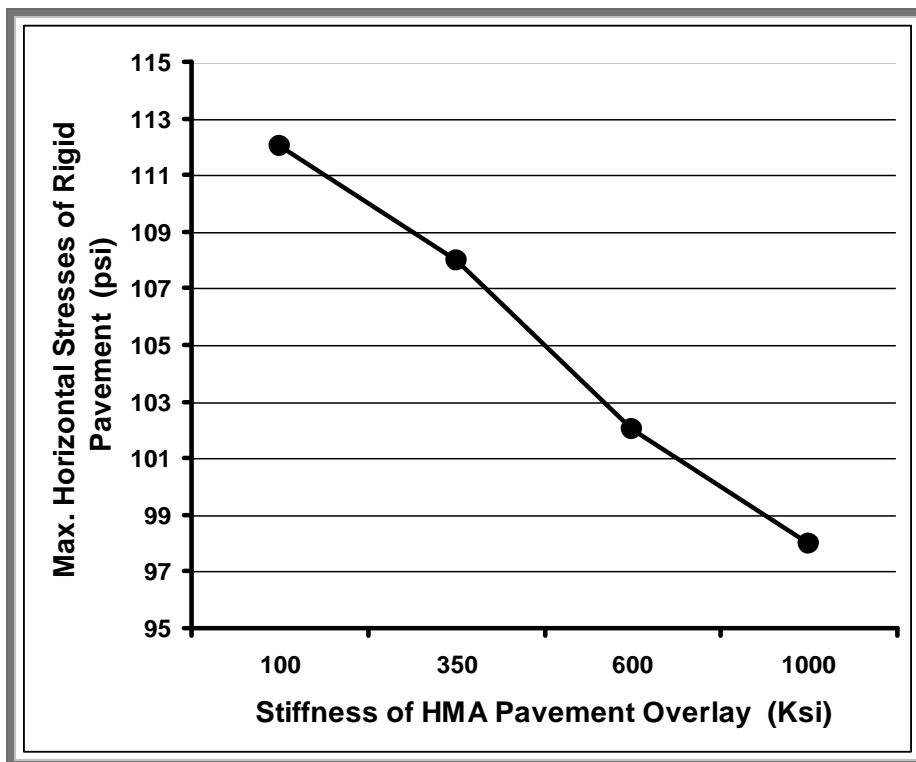
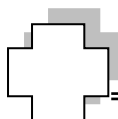


Figure (2.10) Max. Horizontal Stress of Rigid Pavement With Stiffness Variation of the HMA Pavement Overlay (McCullough 1998).



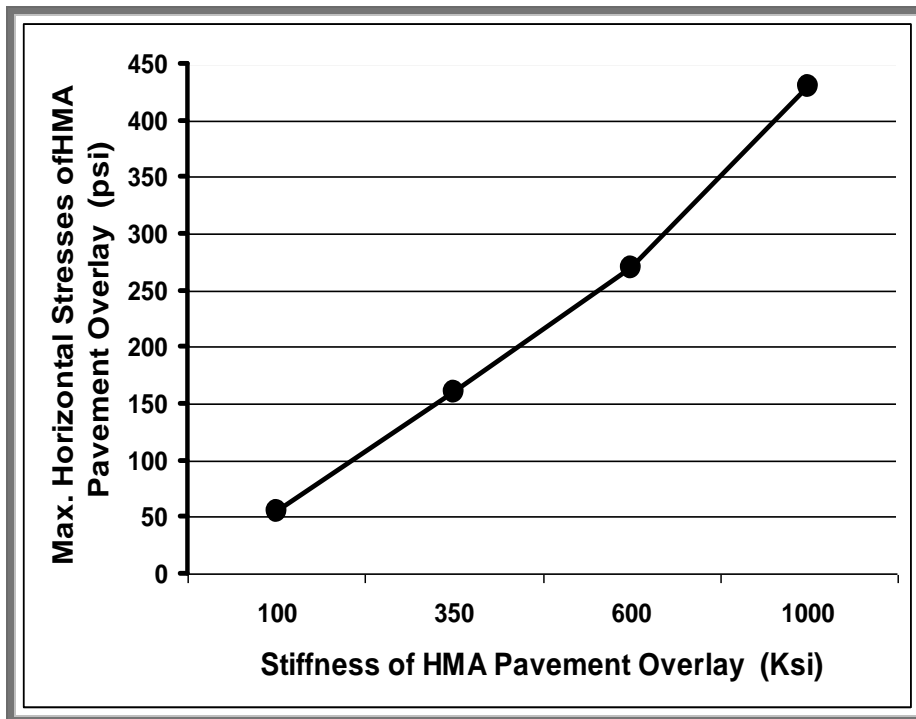
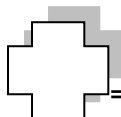


Figure (2.11) Max. Horizontal Stress of HMA Pavement Overlay With Stiffness Variation of the HMA Pavement Overlay (McCullough 1998).

The thickness effect of the HMA pavement overlay on the maximum horizontal stress of rigid pavement is shown in Figure (2.12) which shows that a thicker HMA pavement overlay does help reduce the maximum horizontal stress of rigid pavement that leads to reduce magnitude of horizontal joint movement (i.e. reduces reflective cracking), while the thickness effect of the HMA pavement overlay on the maximum horizontal stress of HMA pavement overlay is shown in Figure (2.13) which shows that a thicker HMA pavement overlay does not help reducing the maximum horizontal stress on the HMA pavement overlay itself (McCullough 1998).



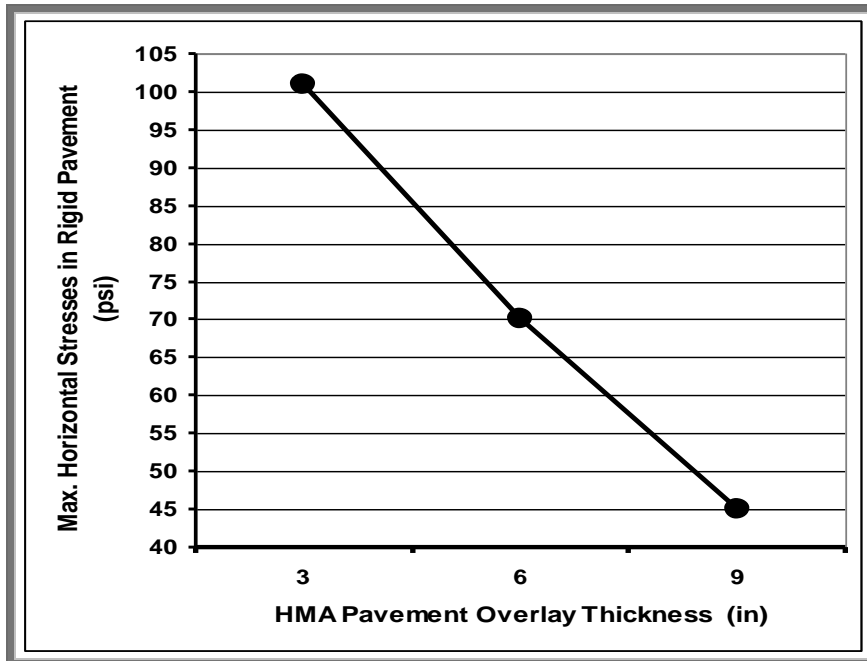


Figure (2.12) Max. Horizontal Stress in Rigid Pavement With Thickness Variation of the HMA Pavement Overlay (McCullough 1998).

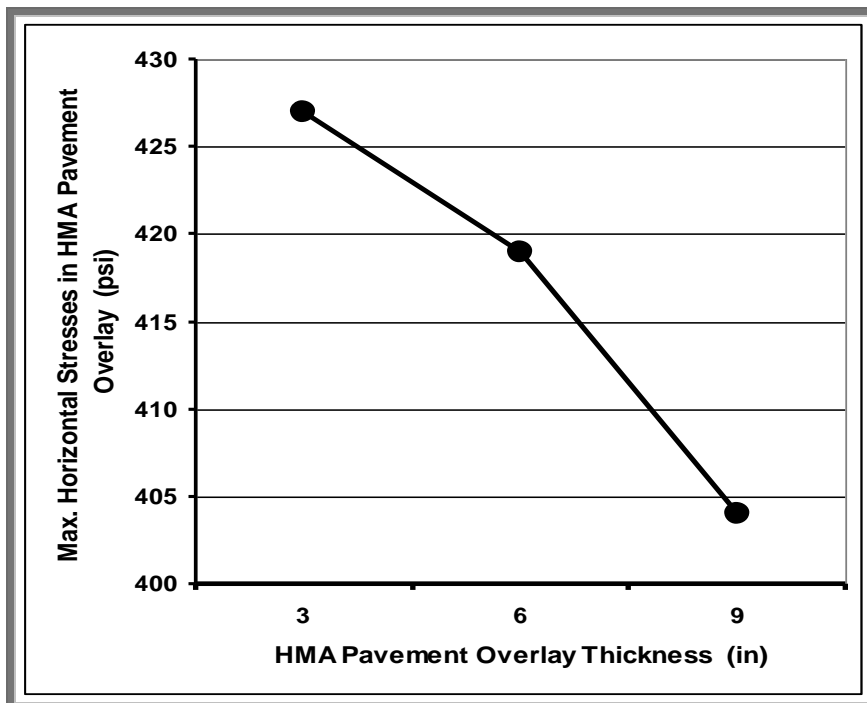
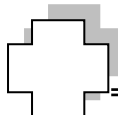


Figure (2.13) Max. Horizontal Stress in HMA Pavement Overlay With Thickness Variation of the HMA Pavement Overlay (McCullough 1998).



2.6.4 Effect of Subgrade Reaction

The tensile stress and compressive stress in the rigid pavement layer increase as the subgrade reaction increases, while the maximum tensile stress in the HMA pavement overlay layer decreases. Stresses in the rigid pavement are not shifted when the pavement has a high value of subgrade reaction. The deflection variation (of the pavement system) for the higher value of subgrade reaction does not differ substantially when compared with the deflection variation for the lower subgrade reaction (**McCullough 1998**).

2.6.5 Effect of Thermal Coefficient of the Rigid Pavement

The thermal coefficient of the rigid pavement is related to the coarse aggregate mixed in the concrete, given that the aggregate consists of about 75% of the total volume (**Neville A. M. 1981**).

The thermal coefficient is known to be affected by the curing of concrete. Generally, air-cured concrete has a thermal coefficient larger than that for wet-cured concrete. Table (2.1) summarized the thermal coefficients for rigid pavements having a typical aggregate type and curing method. Thermal coefficient of the rigid pavement does affect stress distribution of the horizontal stress in both rigid pavement and HMA pavement overlay (**McCullough 1998**).



Table (2.1) Thermal Coefficient of Rigid Pavement as a Function of Aggregate and Curing Method (in./in./F) (Neville A. M. 1981).

| Aggregate | Air cured | Water cured | Air cured and wetted |
|-----------|----------------------|----------------------|----------------------|
| Gravel | 7.3×10^{-6} | 6.8×10^{-6} | 6.5×10^{-6} |
| Limestone | 4.1×10^{-6} | 3.4×10^{-6} | 3.3×10^{-6} |

in./in./°F= 9/5 * mm/mm/°C

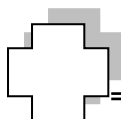
2.6.6 Effect of Age of Pavement

The aging of a pavement structure always affects its service life. The aging is mostly considered to affect the bituminous layers, although the mixing of the unbound materials may be defined as some kind of aging. The bitumen in the asphalt is chemically affected by the continuous influence of the sun, temperature changes and chemicals such as petrol, oil and salt, which results in a harder and less elastic bitumen (Ekdahl 1999).

Anderson et al. (1987) stated that there are two potential causes of age hardening:

1. Loss of the oily components of the asphalt by volatility.
2. Asphalt oxidation by reaction with atmospheric oxygen.

The results of extensive cracking survey, particularly in western Canada as summarized elsewhere (Roads and Transportation Association of Canada, RTAC, 1972) have demonstrated that cracking frequency increases with pavement age. These increases

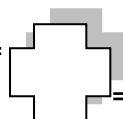


can be caused by an increase in stiffness of the asphalt mix. As well they can be caused by an increasing probability of occurrence of more extreme low and/or variation in temperature, as the pavement becomes older.

2.7 Function of Thin HMA Pavement Overlay

Even though thin HMA pavement overlays do not add any extra structural capacity to the original pavement, it has been proven that properly designed and well-constructed thin HMA pavement overlays do increase the service life of a pavement. The increase in rigid pavement life by thin HMA pavement overlays may be explained by examining its impact on the factors that affect the performance of rigid pavements. Therefore, stress concentrations in rigid pavements caused by factors discussed in the previous sections are one of the primary reasons for accelerated pavement deterioration. Fortunately, many of the factors may be reduced significantly by a thin HMA pavement overlay:

1. A thin HMA pavement overlay may work as an effective barrier to stop moisture from intruding into the pavement structure, thus reducing the potential erosion of the roadbed support resulting from the moisture intrusion.
2. The warping stresses in a rigid pavement may be reduced because the thin HMA pavement overlay helps reduce the vertical temperature differentials along the depth of the rigid pavement



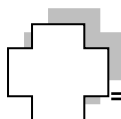
slab. However, asphalt concrete (AC) layers may at times increase the temperature by as much as 10°C, so this needs to be studied in depth.

3. The dynamic loads on rigid pavements may be reduced, because a thin HMA pavement overlay can help provide a smoother pavement surface profile. In addition, the relatively low stiffness of the AC material can also contribute to the reduction of the dynamic loads on the pavements.

It is also worth noting that a thin AC pavement overlay may also have some negative impact on the pavement structure if the overlay is not properly designed and constructed. For example, water may be trapped inside the pavement structure because of the overlay. These issues must be considered when developing the guidelines (Trevino et al. 2004).

2.8 Tensile Strength of The HMA Pavement Overlay Mixtures

Increasing tensile strength has a beneficial effect on minimizing temperature cracking. Several researchers have shown that tensile strength are increased by a reduction in air voids. **Heukelom (1966)** has demonstrated that the tensile strength of the asphalt is related to its stiffness. Since the tensile strength of the asphalt is related to stiffness, the effect of temperature and time of loading on the fracture properties of asphalt of various grades and origins is thus condensed into a single parameter-stiffness. **Heukelom** also suggests that the



tensile strength of an asphalt mixture is a function of stiffness of the asphalt cement contained therein.

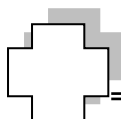
Baladi et al. (2003) reported that the tensile strength of the HMA overlay mixtures are affected by several factors including :

2.8.1 The HMA Pavement Overlay Mix Design

Generally, to improve the ride quality, decrease noise and bleeding, the HMA pavement overlay (surface course) is typically designed to have smaller maximum aggregate size (i.e. higher aggregate surface area) and slightly lower asphalt content relative to other AC courses. The lower asphalt content and smaller aggregate sizes result in thinner asphalt film coating the aggregates and hence, higher stress concentration in the asphalt concrete film. This load to lower overall tensile strength of the HMA overlay. Furthermore, the low asphalt content tends to increase the percent air voids, which also results in low tensile strength.

2.8.2 Temperature and Temperature Gradient Within the HMA Pavement Overlay

It is well known that asphalt binder and asphalt concrete mixture are temperature susceptible materials and their properties including viscosity, elastic modulus and tensile strength vary with temperature. The result of the studies by **Mohammad and Paul (1993)** indicated that the tensile strength of the HMA overlay



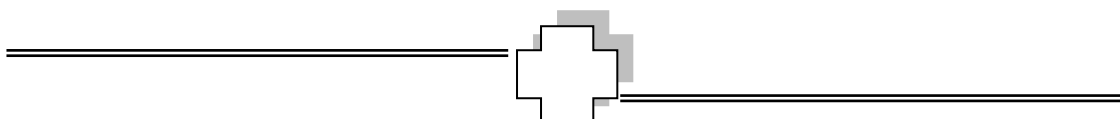
increases as the temperature decreases until the temperature reaches the glass transition point, as the temperature decreases further below this point, the tensile strength of the HMA overlay decreases.

2.8.3 Particle Segregation in the HMA Pavement Overlay

Segregation of the asphalt concrete mixtures may lead to premature distress, such as stripping, rutting, raveling and longitudinal and fatigue cracking. Segregation refers to the separation of coarse and fine aggregates in the asphalt concrete mixtures that based on the motion of segregates. The tensile strength of the HMA overlay increases as the level of particle segregation decreases .

2.8.4 Compaction of the HMA Pavement Overlay

The compaction helps the asphalt film around the aggregates to develop the inter-particle cohesion force. The increase in particle cohesion force results in increasing tensile strength of the HMA overlay.



Chapter 3

Materials and Testing Procedure

The experimental work is limited to the determination of physical properties of asphalt cement and the calculations for the volumetric properties of the asphalt mixture from the Marshall Test specimens. Thereafter, the Pavement Overlay Tester was conducted to investigating the factors related to the resistance of asphalt concrete mixture to reflective cracking.

3.1 Materials

The materials used in this work are locally available in south and middle areas of Iraq. The properties are evaluated according to **American Society for Testing and Materials (ASTM, 2003)** standards compared with the **State Organization of Road and Bridge (SORB, 1982)** specification requirements.

3.1.1 Asphalt Cement

The used asphalt cement was a (40–50) penetration graded from Al- Dourah refinery. The physical properties and tests of the used asphalt cement are shown in Table (3.1).

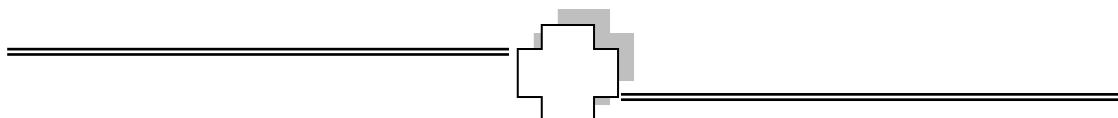
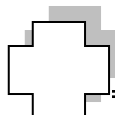


Table (3.1) The Physical Properties and Tests of the Used Asphalt Cement.

| Property | ASTM Designation | Test Result | SORB Specifications |
|---|-------------------------|--------------------|----------------------------|
| Penetration (25 °C, 100 gm, 5 sec), (0.1 mm) | D-5 | 43 | (40 – 50) |
| Kinematic Viscosity at 135 °C, (cst). | D-2170 | 405 | |
| Ductility (25 °C, 5 cm/min). (cm) | D-113 | 107 | > 100 |
| Flash Point (Cleveland open cup) ,(°C) | D-92 | 275 | min. 232 |
| Specific , Gravity at 25 °C | D-70 | 1.055 | |
| After Thin Film Oven Test | | | |
| Penetration of Residue (25 °C, 100 gm, 5 sec) | D-5 | 33 | |
| Ductility of Residue, cm,(25°C,5 cm/min) | D-113 | > 20 | |



3.1.2 Aggregate

The source of the aggregate used in this work was Al-Niba'ee quarry. This aggregate is widely used in south and middle areas for asphalt works. Three gradations were selected for aggregate with a maximum size of 9.5mm using different percentages of filler as shown in Table (3.2). The physical properties are summarized in the Table (3.3).

3.1.3 Filler

In this study, three types of mineral filler have been used including: limestone dust, hydrated lime, and ordinary Portland cement. They were brought from lime factory in Karbala governorate. The physical properties of these three types are presented in Table (3.4).

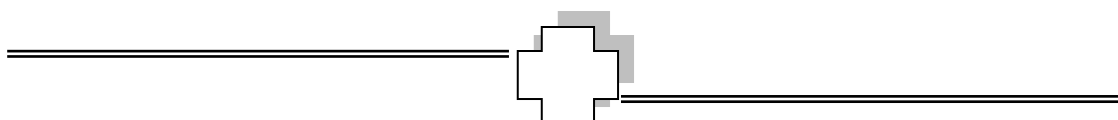


Table (3.2) Asphalt Mixture Gradings.

| Sieve | | Gradings of Surface (Wearing) Course (% Passing by Weight of Total Aggregate + Filler) | | | Specification Limits SORB |
|---|----------------------|---|--------------------------|------------------------|--|
| | | Upper Limit | Average Limit | Lower Limit | |
| Opening (mm) | Size (in) | | | | |
| 12.5 | 1/2 | 100 | 100 | 100 | 100 |
| 9.5 | 3/8 | 100 | 95 | 90 | 90-100 |
| 4.75 | No.4 | 85 | 70 | 55 | 55-85 |
| 2.36 | No.8 | 67 | 50 | 32 | 32-67 |
| 300 um | No.50 | 23 | 15 | 7 | 7-23 |
| 75 um | No.200 | 10 | 7 | 4 | 4-10 |
| Asphalt Cement (% weight of total mix) | | 4-6 | 4-6 | 4-6 | 4-6 |

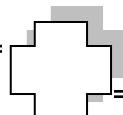
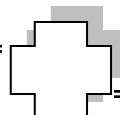


Table (3.3) Physical Properties of the Used Aggregate.

| Property | ASTM Designation | Course Aggregate | Fine Aggregate |
|----------------------------------|----------------------------------|-------------------------|-----------------------|
| Bulk Specific Gravity | C-127 & C-128 | 2.63 | 2.63 |
| Apparent Specific Gravity | C-127 & C-128 | 2.76 | 2.68 |
| % Water Absorption | C-127 & C-128 | 2.8 | 0.5 |

Table (3.4) Physical Properties of the Used Types of Filler.

| Property | Filler Type | | |
|--|-----------------------|---------------|----------------------|
| | Limestone Dust | Cement | Hydrated Lime |
| Specific Gravity | 2.67 | 3.1 | 2.76 |
| Passing Sieve No.200 (0.075 mm) | %94 | %95 | %97 |



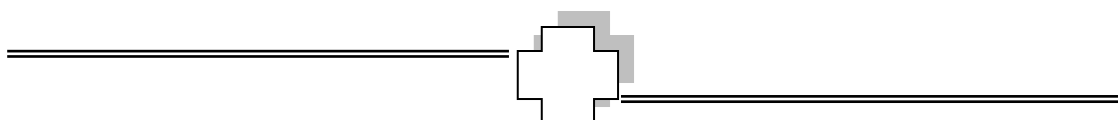
3.2 Methods of Testing

3.2.1 Marshall Test

This test was carried out according to the **ASTM (D1559)** which covers the measurement of the resistance to plastic flow of cylindrical specimens of bituminous paving mixture loaded on the lateral surface of the specimen by means of Marshall Apparatus shown in Figure (3.1). The Marshall stability is the maximum load the specimen can withstand before failure when tested in the Marshall stability test. The configuration of the Marshall stability test is close to that of the indirect tensile strength test, except for the confinement of the Marshall specimen imposed by the Marshall testing head. Thus, the Marshall stability is related to the tensile strength of the asphalt mixture.

The Marshall flow is the total vertical deformation of the specimen, in units of 0.01 in., when it is loaded to the maximum load in the Marshall stability test. The Marshall flow can provide some indication of the resistance of an asphalt mixture to plastic deformation. Mixtures with low flow number are stiff and may be difficult to compact. However, these mixtures are more resistance to rutting than those with high flow numbers.

The percent of aggregate, percent of binder, percent air voids, stability, and flow were found for each prepared specimen, using ASTM standard methods. The Marshall stiffness was also determined



for these specimens. The result and calculations are presented in chapter Four.

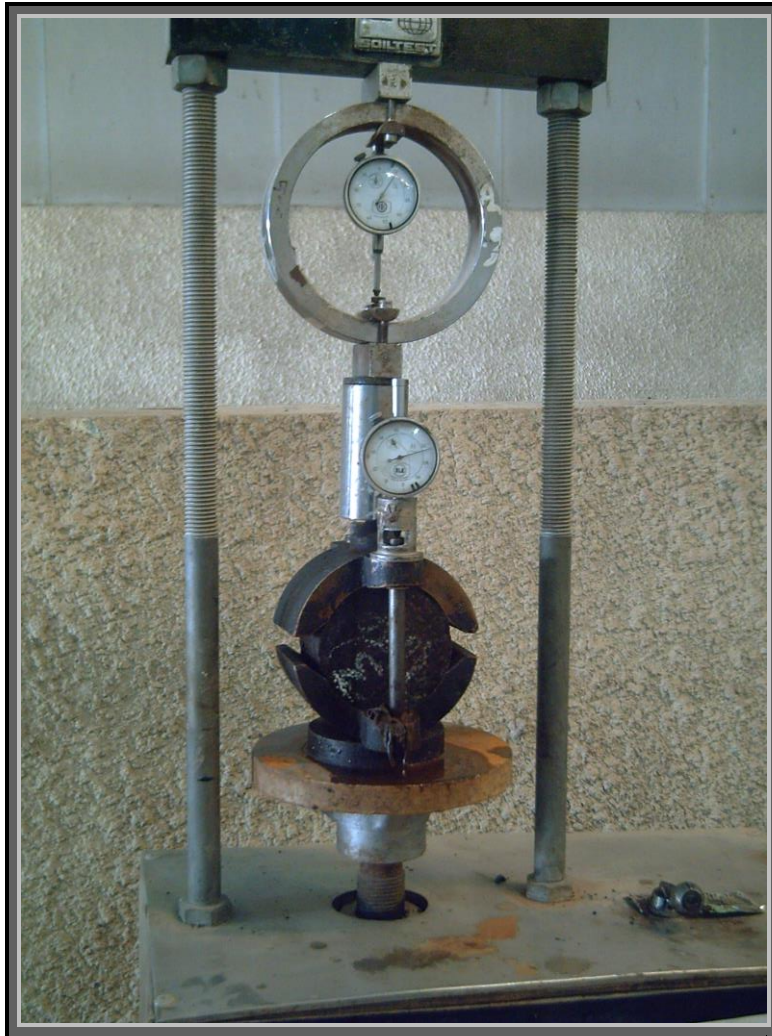
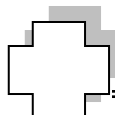


Figure (3.1) Marshall Apparatus.

3.2.2 Pavement Overlay Tester (POT)

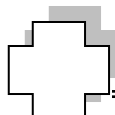
The Pavement Overlay Tester (POT) shown in Figure (3.2) has been manufactured locally for this work in accordance with the requirements of Texas Transportation Institute (Appendix A).



The Objective of POT is to prepare a suitable apparatus which can be routinely used by engineers to measure the reflective cracking resistance of asphalt concrete mixtures by simulating the opening and closing of joints in rigid pavements due to temperature variations.



Figure (3.2 a) Pavement Overlay Tester (POT).



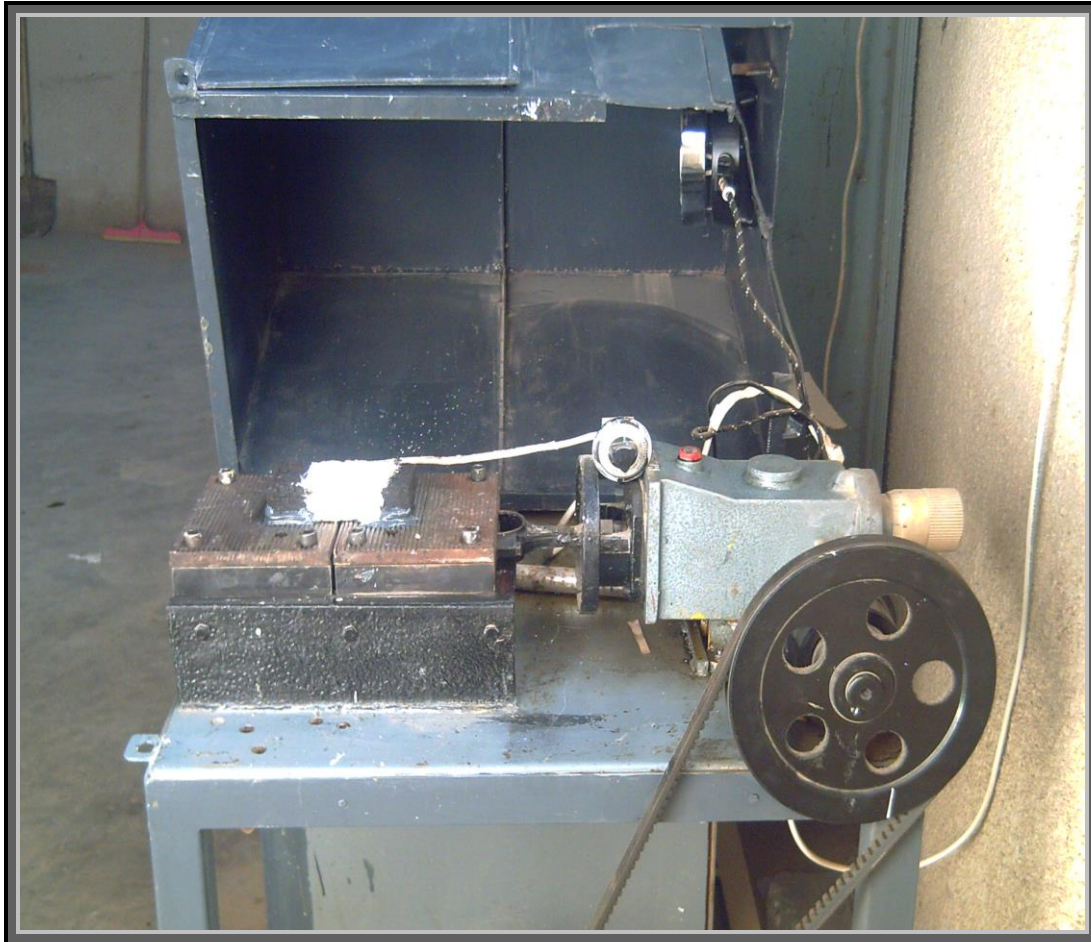


Figure (3.2 b) Pavement Overlay Tester (POT).

In order to overcome the difficulties in the previous overlay testers related to the fabrication of large beam samples (750×250)mm, Texas Transportation Institute had suggested the use of smaller test samples (Figure 3.3) (150×75) mm making the overlay testing easier (Zhou and Scullion 2005).

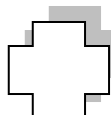
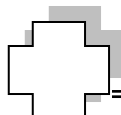




Figure (3.3) The Used Samples in Test.

Furthermore, the three-dimensional finite element program, ABAQUS, was used to analyze the stress distribution of different sizes of specimens. For example, as shown in Figure (3.4), the main tensile stress of asphalt concrete is limited to the middle 2.5 in (63.5mm) part of specimen. This means that the end effect has little influence on the overlay testing results. Therefore, it is reasonable to use 6 in (150 mm) long specimens in the overlay tester. The proposed small specimen size makes the overlay testing more practical and easier to use, since this size specimen can be readily fabricated in the lab by the engineer (Zhou and Scullion 2005).

Finally, the apparatus (POT) had locally been manufactured as possible as the technical capabilities available in Babylon governorate could with 70 days are duration of fabricating the device and cost of fabricating the device is 750000 Iraqi Dinar.



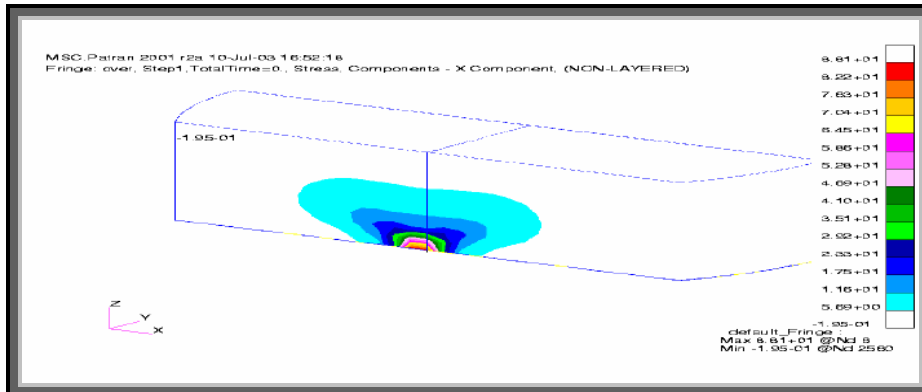


Figure (3.4) Tensile Stress Distribution of Asphalt Concrete Under 0.381mm (0.015in) Opening Displacement (Zhou and Scullion 2005).

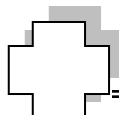
3.2.2.1 Parts of the Pavement Overlay Tester

Testing machine:

A mechanical testing machine driven by an electric motor through a gear box capable of providing a movable displacement (0-7) mm. The testing machine has a capability of applying load of 2 hp.

Environmental chamber:

The environmental chamber (made by using thin steel plate) is capable of controlling the temperature of specimens over a temperature range from (0-75) $^{\circ}$ C. The environmental chamber consists of heater to provide the required temperature for specimens and fan to distribute the air inside the chamber. This chamber keeps the required temperature for test by using a thermostat. The chamber is large enough to accommodate the test specimen glued to plates by epoxy (see Figure 3.2).



Plates:

The steel plates have the dimensions of 300mm×150mm×10mm are shown in Figure (3.5). Grooves are cut in plates at regular intervals (1.5mm deep by 3mm wide at 6mm interval) to providing fully bonding between the plates and specimens by using epoxy.

The maximum opening of plates (spacing between plates) depends upon test temperature (maximum opening is 2mm when the test temperature 25°C) (Zhou and Scullion, 2005).

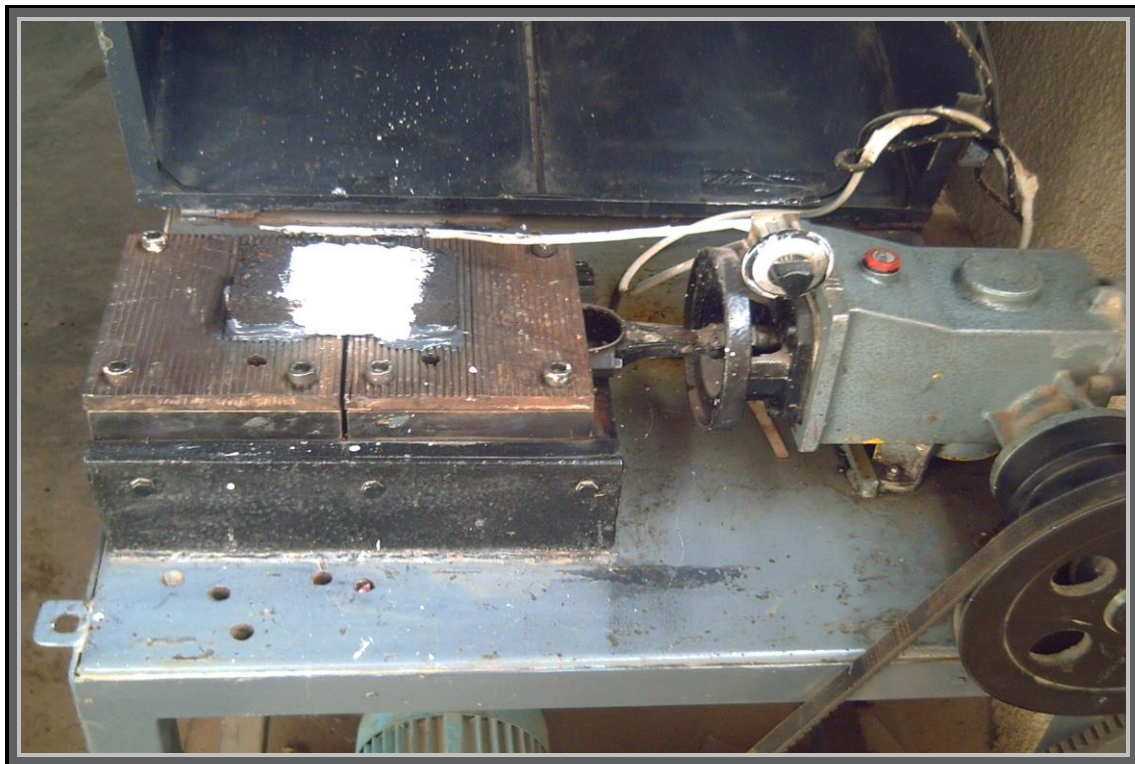
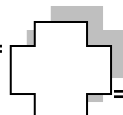


Figure (3.5) Parts of Pavement Overlay Tester.

Sample Size:

Beam samples of HMA mixture with dimensions of 150mm× 75mm ×30mm .



Loading Rate and Opening Displacement of Plate

The loading rate of movable plate is 6 rotations per minute. The opening displacement of plates is determined based on the following assumption and calculations:

- Daily temperature variation (ΔT): 25 °C.
- Slab length (L): 5m.
- Coefficient of thermal expansion of rigid pavement (α): 11×10^{-6} mm/mm/°C.
- Coefficient of resistance (c): 0.7.

Opening displacement of plate = $\Delta t \times L \times \alpha \times c$

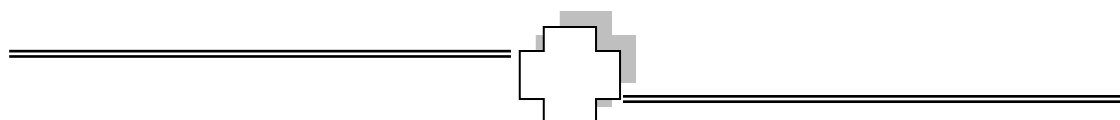
$$= 25 \times 5 \times 1000 \times 11 \times 10^{-6} \times 0.7 = 1 \text{ mm.}$$

The opening displacement of POT plates is 1 mm (0.0394 in).

3.3 Properties of Asphalt Concrete Mixtures

In this study, the properties of asphalt concrete mixtures used in testing (Marshall Test and POT Test) are:

- Asphalt Cement Grade = (40-50).
- Aggregate maximum mineral size = 9.5 mm (3/8").
- Mixing Temperature = 160 °C.
- Compaction Temperature = 135 °C.



The testing variables for asphalt concrete mixtures include the following:

- Test Temperature, $T = (5, 25, 40 \text{ and } 55) \text{ } ^\circ\text{C}$.
- Open Displacement, $\text{OD} = (1, 2 \text{ and } 3.5) \text{ mm}$.
- Asphalt Content, $\text{AC}\% = (4.1, 4.7, 5.2 \text{ and } 6) \%$.
- Filler Type = (Limestone, Hydrated Lime and Cement).
- Gradation: (Fine, Intermediate, and Coarse).
- The Sample Thickness, $t = (25 \text{ and } 30) \text{ mm}$.

3.4 Testing Program & Preparation of Specimens

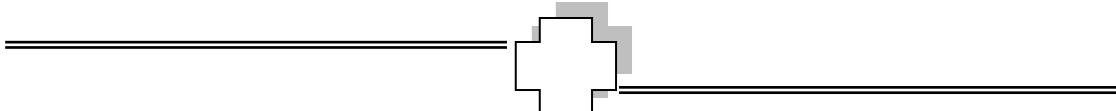
In this work, 115 overlay specimens are prepared and tested in the Transportation Lab of Babylon University.

3.4.1 Marshall Test

Marshall Specimen (sample (A) that shown in Table 4.1 of chapter four) is prepared with dimension of 63.5mm in height and 101.6mm in diameter with a total weight of about 1200gm.

The following steps were performed for the preparation of the sample (A):

- The combined aggregate with filler were heated to 160°C in controlled electric oven.
- The asphalt (4.7% by weight of total mix) was heated up to about 160°C in controlled electric oven and then mixed with the



corresponding gradation of heated aggregate and filler, and the final mix was put in the mold.

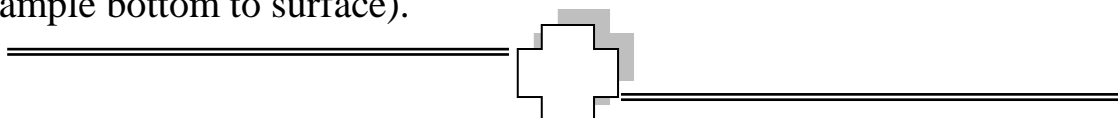
- The specimen was then compacted (at 135⁰C) using Marshall compaction method (hand compaction) with 75 blows each face.

3.4.2 Pavement Overlay Tester

Test specimens are prepared with dimension of 150mm (6in) in length, 75mm (3in) in width and 30mm (1.2in) in height with a total weight around 775gm. The specimens formulated were then compacted using Marshall compaction method (hand compaction) with 48 blows each face. Then each specimen was epoxied to two steel plates (with half the length of the specimen resting on each plate) and allowed to cure for 15 hours.

To represent an existing joint (or crack) in underlying pavement, the two steel plates were separated by 2 mm under the center of the specimen. The gap (spacing between plates) was covered with clear adhesive tape to prevent the epoxy resin from entering. The compacted specimen was then spanned across the gap and epoxy in place. Each specimen was painted white in the area where cracking was most likely to occur. This technique enhanced the visibility and detection of cracks during the testing phase.

Three specimens were compacted for each of the variables mentioned in section (3.3) and a digital camera had been used to control recording the exact time of failure (time of crack propagation from sample bottom to surface).

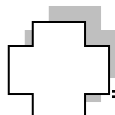


The repeated loading is applied until failure. The loading rate with opening displacement is used to determine the reflective cracking life N_{RCL} of asphalt concrete mixtures. Figure (3.6) shows the POT with specimen glued to the test plates.

The number of cycles to crack propagation from sample bottom to surface (N_{RCL}) = Time of failure (minute) \times 6 rotation per minute.



Figure (3.6) POT with Specimen Glued to the Test Plates.



4.1 Properties of Used Samples

The different mixture variables used in this study are shown in Table (4.1). The volumetric properties of asphalt concrete mixtures are shown in Table (4.2).

Table (4-1) Different Mixture Variables Used in the Work.

| Sample | | A | B | C | D | G | J | M | P |
|---------------------|------------------------|---|---|---|---|---|---|---|---|
| Asphalt Content | AC = 4.1 % | | | | | | 0 | | |
| | AC = 4.7 % | 0 | 0 | 0 | 0 | 0 | | | |
| | AC = 5.2 % | | | | | | | 0 | |
| | AC = 6 % | | | | | | | | 0 |
| Filler Type | Limestone Filler | 0 | | | 0 | 0 | 0 | 0 | 0 |
| | Portland Cement Filler | | 0 | | | | | | |
| | Hydrated Lime Filler | | | 0 | | | | | |
| Gradation Limit | Fine Gradation | | | | | 0 | | | |
| | Intermediate Gradation | 0 | 0 | 0 | | | 0 | 0 | 0 |
| | Coarse Gradation | | | | 0 | | | | |
| No. of Test Samples | | 5 | 3 | 3 | 3 | 3 | 3 | 3 | 3 |

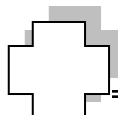
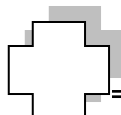


Table (4-2) The Volumetric Properties of Asphalt Concrete Mixtures.

| Sample | Bulk Gravity (gm/cm³) | Theoretical Gravity (gm/cm³) | % Air Voids |
|---------------|---|--|------------------------|
| A | 2.34 | 2.435 | 4.72 |
| B | 2.33 | 2.429 | 4.1 |
| C | 2.322 | 2.438 | 4.75 |
| D | 2.333 | 2.45 | 4.8 |
| G | 2.348 | 2.446 | 4 |
| J | 2.302 | 2.422 | 4.95 |
| M | 2.371 | 2.465 | 3.8 |
| P | 2.399 | 2.476 | 3.1 |



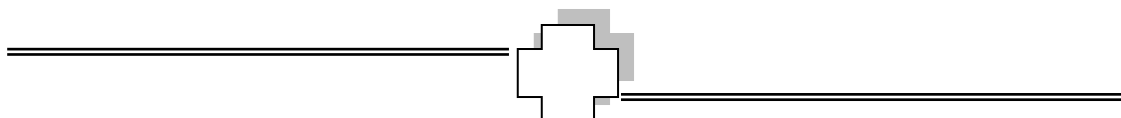
4.2 Influence of Different Variables

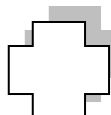
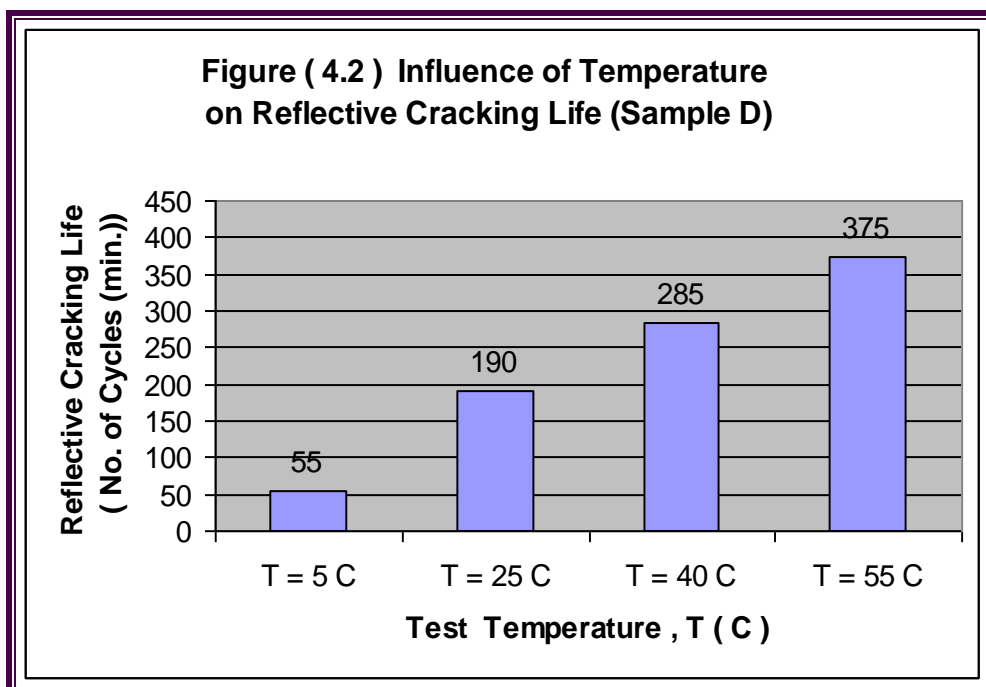
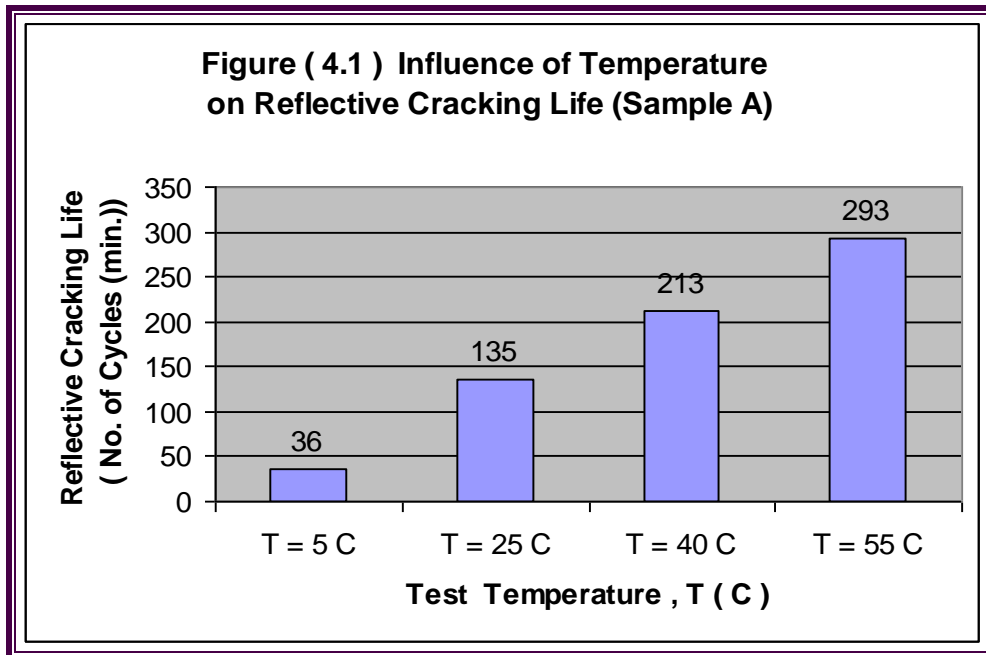
The variables investigated in this study include test temperature, open displacement of plates, asphalt content, filler type, selected gradation, and sample thickness.

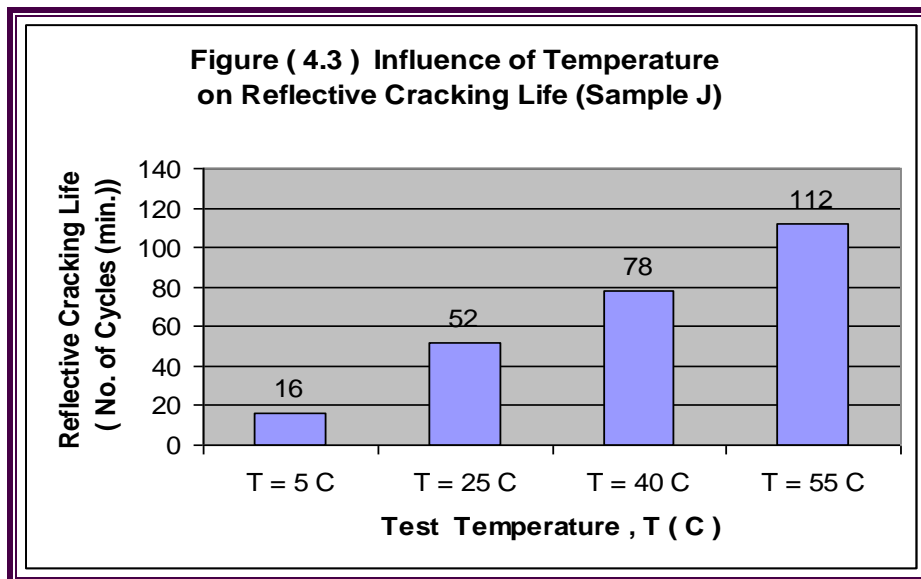
4.2.1 Influence of Temperature on Reflective Cracking Life

It is well known that the temperature is the major contributor to reflective cracking of HMA overlays. POT testing was conducted at four temperatures: (5, 25, 40, and 55) °C respectively. The opening displacement of plates was 1mm (0.0394 in) for all temperature.

The averaged results of reflective cracking life for sample (A) are presented in Figure (4.1), in Figure (4.2) for sample (D), and in Figure (4.3) for sample (J). It is clear from these figures that the temperature had significant influence on the reflective cracking life because the asphalt mixture with higher temperature becomes more flexible and more able to absorb the horizontal strain in the bottom of the HMA overlay resulted from temperature variation of rigid pavement. The test results were agreed with the **Zhou and Scullion (2005)** study.



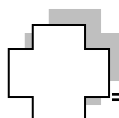


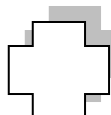
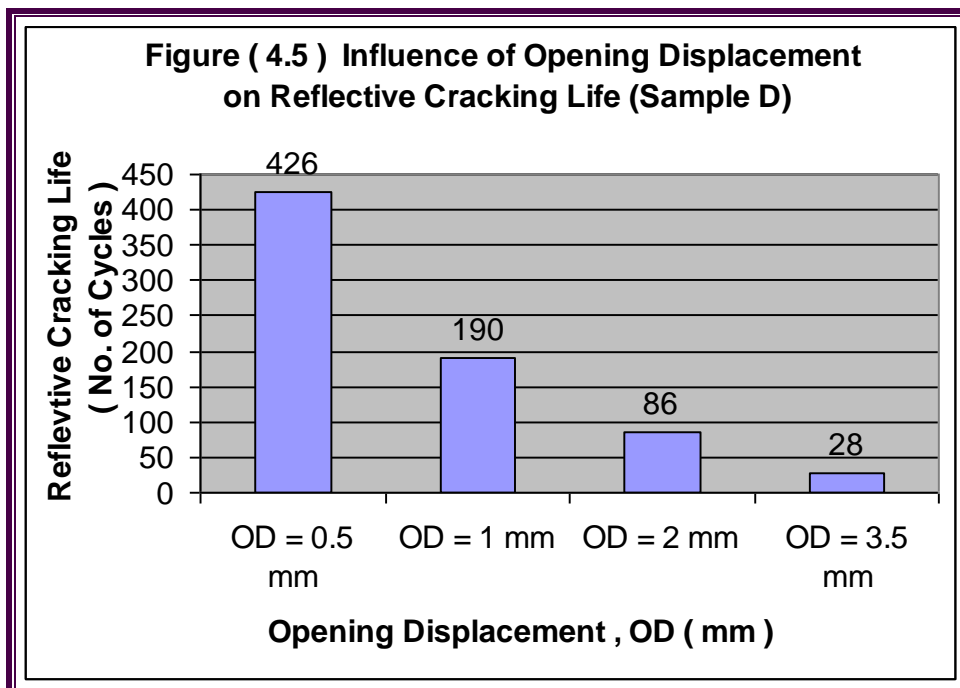
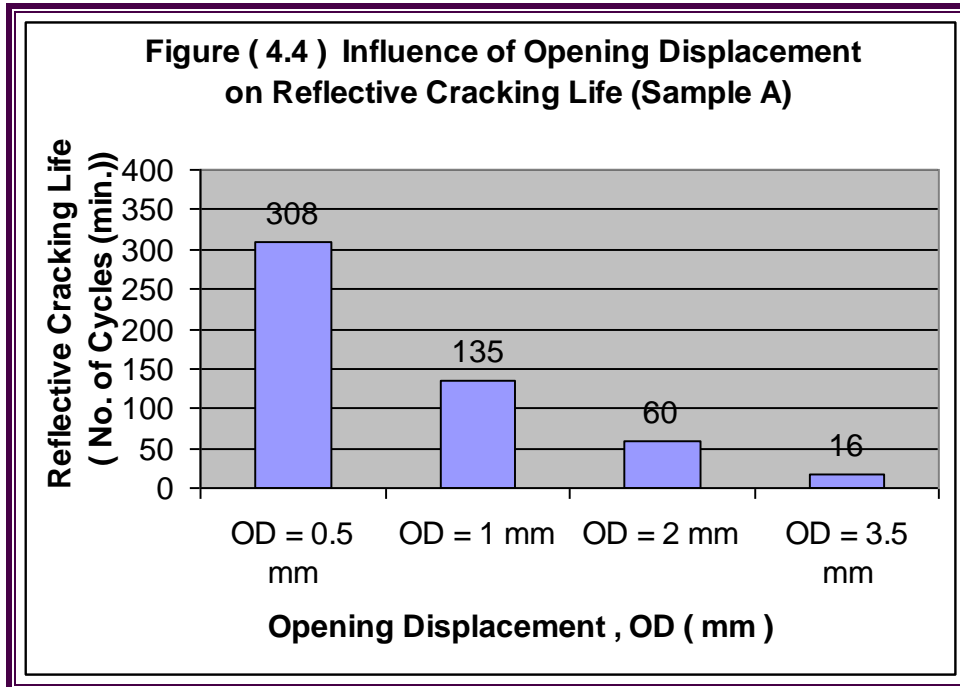


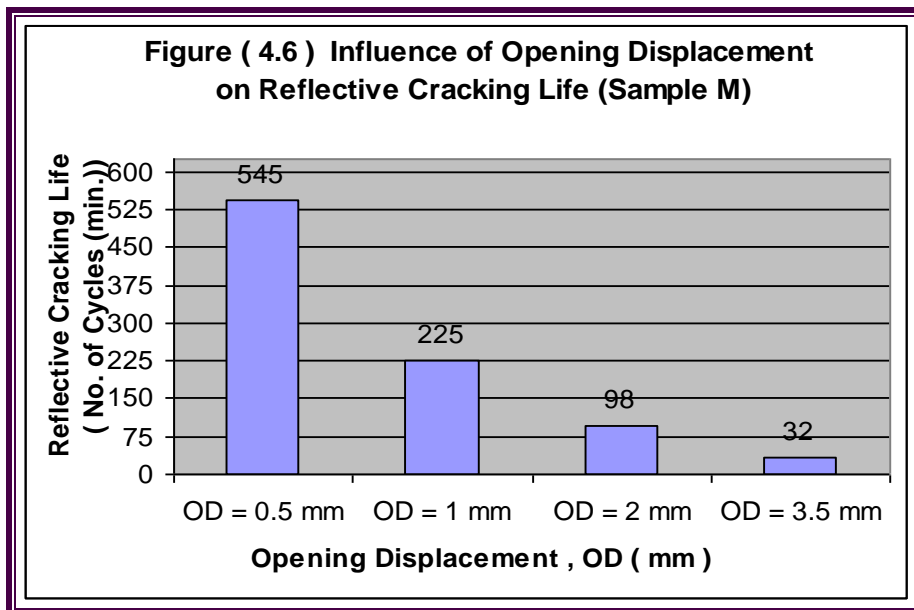
4.2.2 Influence of Opening Displacement on Reflective Cracking Life

The temperature variation or opening displacement (OD) of plates is another major factor affecting the reflective cracking. POT testing was conducted at 25 °C and the opening displacement of plates (OD) was: (0.5, 1, 2, and 3.5) mm.

The averaged results of reflective cracking life for sample (A) are presented in Figure (4.4), in Figure (4.5) for sample (D), and in Figure (4.6) for sample (M). It can be seen from these figures that with the increasing of opening displacement (OD), the reflective cracking life of asphalt mixture decreases because larger opening displacement means higher temperature variation and so a higher horizontal strain in the HMA overlay, which resulted in a lower reflective cracking life. **Zhou and Scullion (2005)** study had reported a similar results.





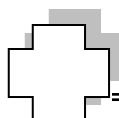


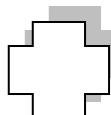
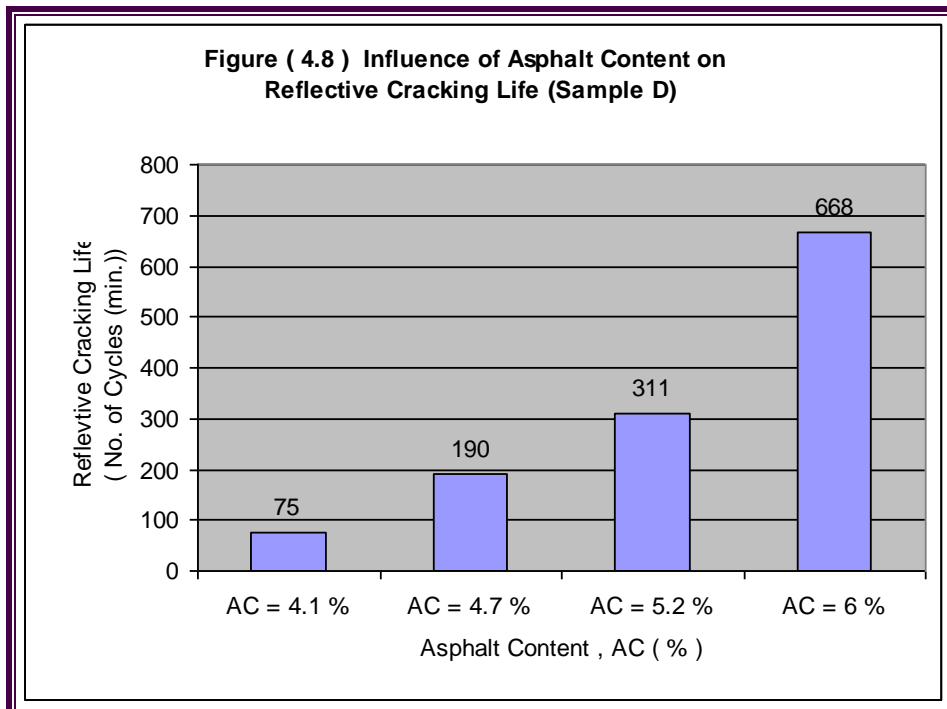
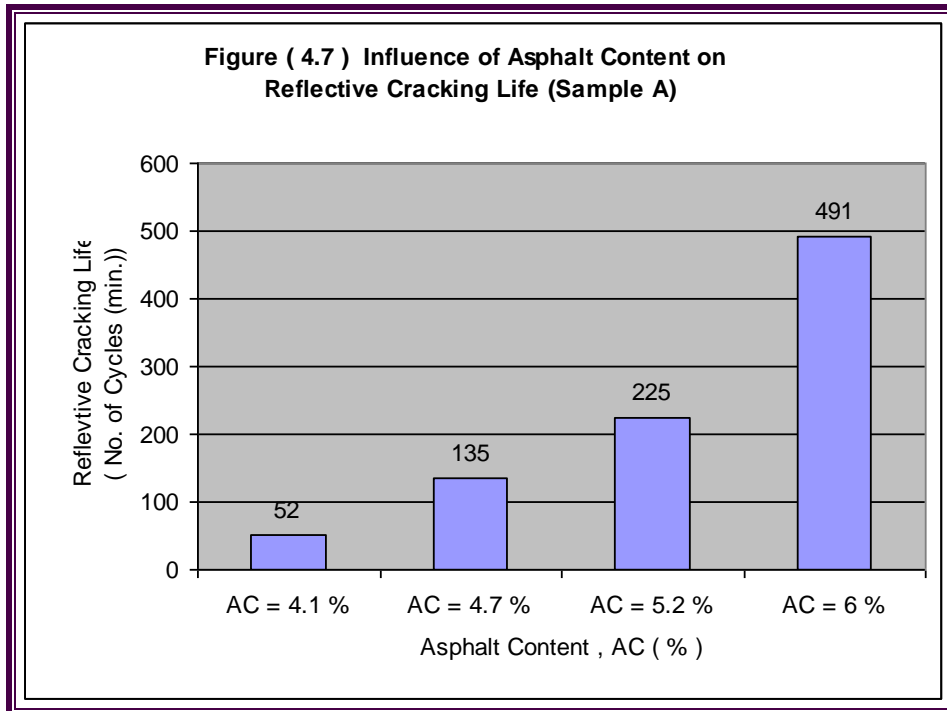
4.2.3 Influence of Asphalt Content on Reflective Cracking Life

The four asphalt content (AC) used were (4.1, 4.7, 5.2, and 6) % respectively. The POT testing was conducted at 25 °C (77 °F) and 1mm (0.0394 in) opening displacement of plates. The averaged results of reflective cracking life for sample (A) are presented in Figure (4.7), in Figure (4.8) for sample (D).

It can be seen from these figures that with the increase of asphalt content (AC), the reflective cracking life of the asphalt mixture significantly increases.

It is clear from the equation (2.6) and the paragraph in page (19) that more asphalt content in the mixture asphalt, the smaller the A parameter and therefore the greater the reflective cracking life and the test results were agreed to the **Zhou and Scullion (2005)** study.

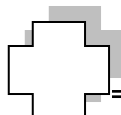
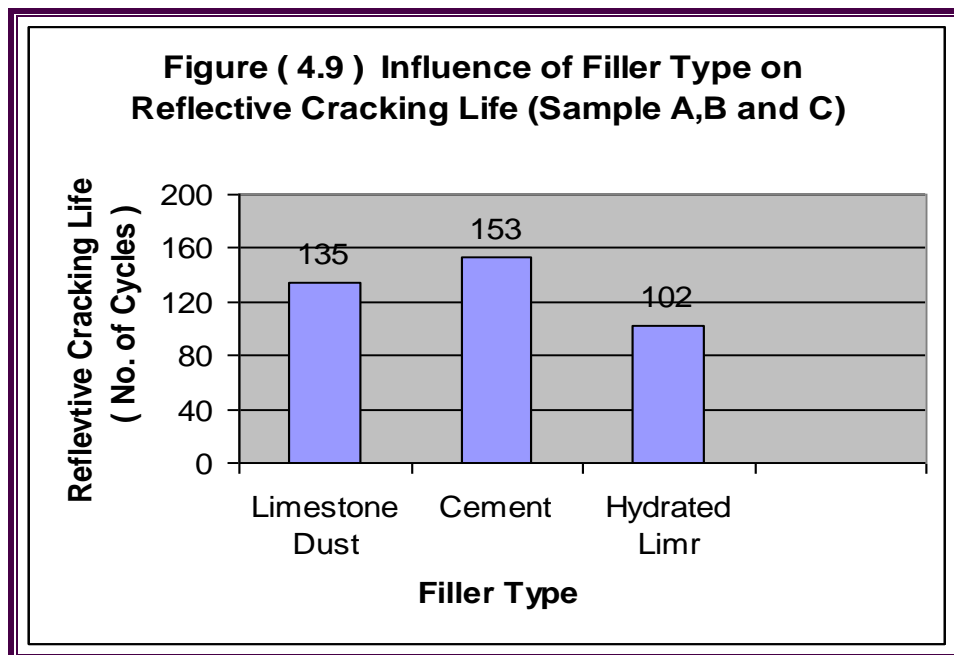




4.2.4 Influence of Filler Type on Reflective Cracking Life

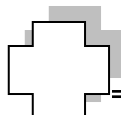
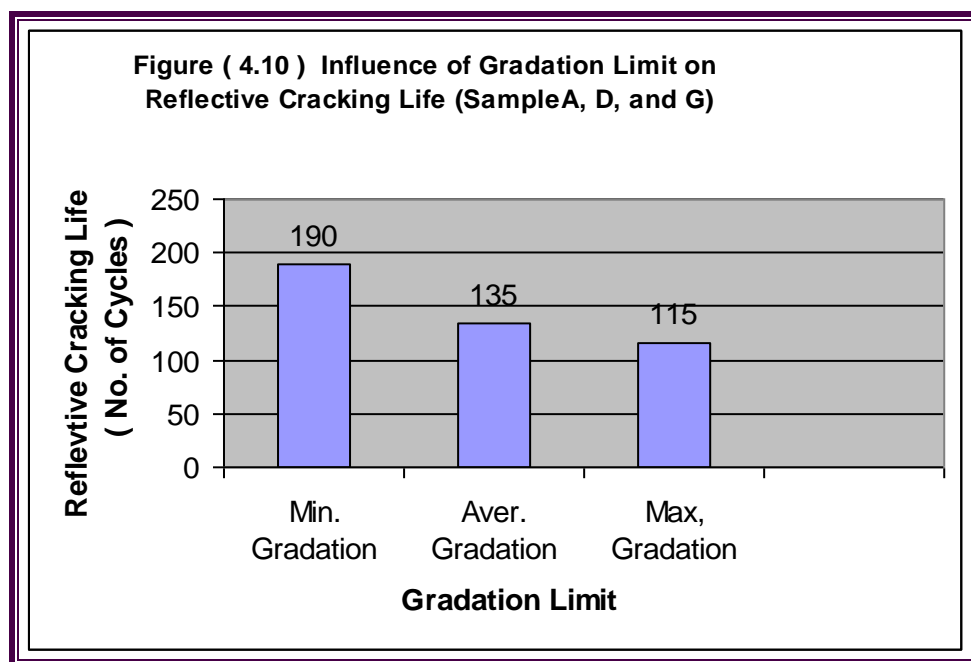
The three filler types used were: limestone dust, cement, and hydrated lime respectively. The POT testing was conducted at 25 °C (77 °F), 1mm (0.0394 in) opening displacement of plates, and 4.7% asphalt content. The averaged results of reflective cracking life for samples (A, B, and C) are presented in Figure (4.9).

It is clear from the Table (4.2), the asphalt mixture with Portland cement as a mineral filler has less air void compared with the mix with hydrated lime or limestone dust, and from equation (2.6) the smaller air void, the lower A parameter and therefore longer reflective cracking life.



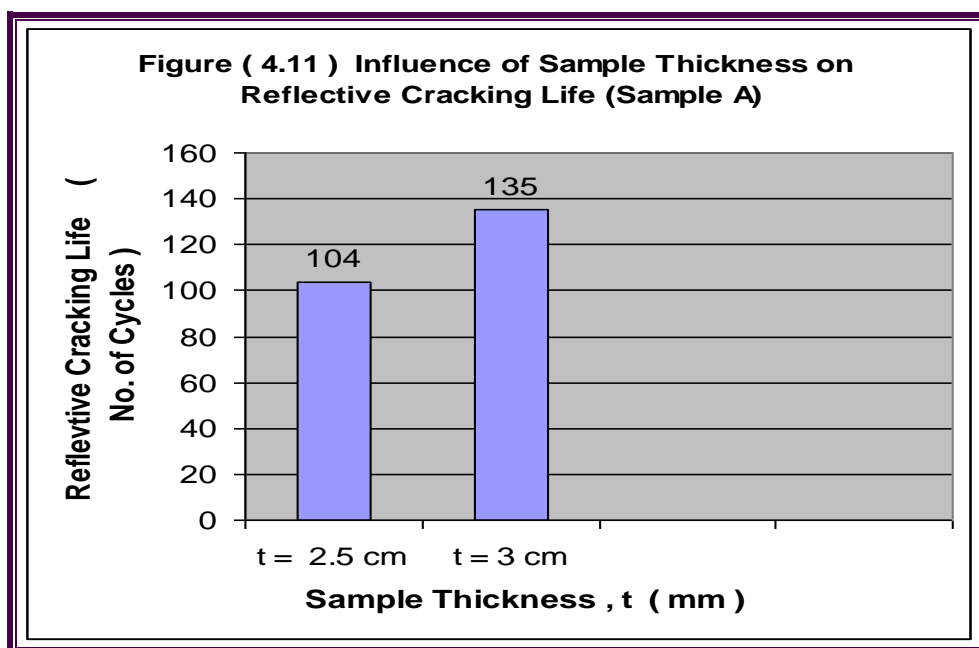
4.2.5 Influence of Gradation Limit on Reflective Cracking Life

The POT testing was conducted at 25 °C (77 °F) and 1 mm (0.0394 in) opening displacement of plates. The averaged results of reflective cracking life for sample (A) are presented in Figure (4.10). From test results, the coarse graded mixture (lower gradation limit) of asphalt concrete mixtures has more resistance to reflecting cracking because the mix has less air void.



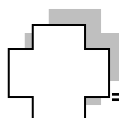
4.2.6 Influence of Sample Thickness on Reflective Cracking Life

The POT testing was conducted at 25 °C (77 °F) and 1 mm (0.0394 in) opening displacement. The averaged results of reflective cracking life for sample (A) are presented in Figure (4.11). An increased resistance to reflective cracking has been obtained for thicker mixes. This behavior seems to be similar to that reported by others researchers (Gulden and Brown (1985), Predoehl (1989) and Finn and Monismith (1984)).



4.2 Marshall Test Results

Result of Marshall Test for sample A (main mix) was: Stability (1010kg), Flow (3.5mm) and Marshall Stiffness (288 Kg/mm).



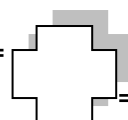
Chapter 5

Conclusions and Recommendations

5.1 Conclusions

Within the limitations of materials and testing program adopted in this work, the following are concluded:

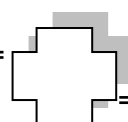
1. The increase of pavement temperature causes more resistance to reflective cracking.
The number of opening and closing cycles has been increase by 210% for an increase in temperature from 25°C to 55°C.
2. Decreasing the opening and closing displacements of joints from 1mm to 0.5mm has increased the number of cycles for the initiation of reflective cracking by 231%.
3. Increasing asphalt content of paving mixtures from 4.7% to 5.2% causes an increased resistance to reflective cracking with an increased number of cycles by 166%.
4. Replacing the limestone dust by portland cement as mineral filler in asphalt overlays has increased the number of cycles for reflective cracking by 113%.



5. Coarse gradation causes an increased resistance to reflective cracking with an increased number of cycles by 141% for a nominal max. aggregate size of 9.5mm.
6. Thicker asphalt concrete overlays provide more resistance to reflective cracking.
7. The locally manufactured Pavement Overlay Tester (POT) which is determined to be as a suitable mean to evaluate reflective cracking resistance of paving mixtures in short duration with easy handling, is recommended to be used for this purpose (up to 30mm thickness).

5.2 Recommendations

1. It is recommended to modify the Pavement Overlay Tester (POT) to increase the thickness of HMA overlay specimen to more than 30mm to simulate the actual pavement thickness.
2. It is also recommended to evaluate the influence of asphalt cement rheological properties, chemical composition and the use of polymer additives on the resistance of asphalt overlays to reflective cracking measure by using the manufactured Pavement Overlay Tester (POT).



References

- Ahmed, N. G. **"The Development of Models for the Prediction of Thermal Cracking in Flexible Pavements "**, Ph.D Thesis, University of Baghdad, 2003.
- Anderson, D. A., Marasteanu, M. O., Chapiion-Lapalu, L., Le Hir, Y., Martin, D. and Planche, J. P., **"Low-Temperature Thermal Cracking of Asphalt Binders as Ranked by Strength and Fracture Properties"**, Proceedings of 2nd Eurasphalt & Eruobitume Congress, pp.7, 2000.
- Anderson, D. A., Petersen, J. C., and Christensen D. W. **"Variation in Asphalt in Asphalt Cement and Their Effects on Performance of Asphalt Concrete Mixture"**, Proceedings Association of Asphalt Paving Technologists, Vol. 56, pp. 250, 1987.
- ASTM, American Society of State Highway and Transportation Officials, 2003.
- Baladi, G. Y., Schorsch, M. and Svasdisant, T., **"Determining the Causes of Top-Down Cracks in Bituminous Pavements"**, Michigan Department of Transportation, Michigan Asphalt Paving Association, 2003.



References

- Barksdale, R.D., "**Fabrics in Asphalt Overlays and Pavement Maintenance**", NCHRP Synthesis 171, National Cooperative Highway Research Program, National Research Council, Washington, D.C., 1991.
- Bayomy F. M., Al-kandari F. A. and Smith R. "**Mechanically Based Flexible Overlay Design System for Idaho**", Transportation Research Record 1543, Transportation Research Board, Washington, D. C., pp. 10-19, 1996.
- Blankenship, P., Iker, N., and Drbohlav, J., "**Interlayer and Design Considerations to Retard Reflective Cracking** ", Annual Meeting of the Transportation Research Board, 2002.
- Brooker T., Foulkes M. N. and Kennedy C. K., "**Influence of Mix Design of Reflection Cracking Growth Rates Through Asphalt Surfacing**", 6th International Conference on Structural Design of Asphalt Pavements, Vol. 1, University of Michigan, pp. 107, 1987.
- BRRC, Belgian Road Research Center, "**The Design of Flexible Road Pavements with Bitufor Under Traffic Loading**", Report EP 5035/3744, Brussels, Belgium, 1998.
- Button, J.W., Estakhri, C. K. and Little, D. N., "**Hot In-Place Recycling of Asphalt Concrete**", NCHRP Synthesis of Highway Practice 193. TRB, National Research Council, Washington, D.C, pp. 69, 1994.



References

- Champion-Lapalu, L., Planche, J.P., Martin, D., Anderson, D. A. and Gerard, J. F., "**Low-Temperature Rheological and Fracture Properties of Polymer-Modified Bitumens**", Proceedings of 2nd Eurasphalt and Eurobitume Congress, pp. 122, 2000.
- Choubane, B., and Mang, T., "**Nonlinear Temperature Gradient Effect on Maximum Warping Stresses in Rigid Pavements**", TRR 1370, 1992.
- Cleveland, G. S., Button, J. W. and Lytton, R. L., "**Geosynthetics in Flexible and Rigid Pavement Overlay Systems to Reduce Reflection Cracking**", Texas Department of Transportation and the U.S. Department of Transportation, Federal Highway Administration, Report No. 1777-1, pp. 5-13, 2002.
- Decker, D. S. and Hansen, K. R., "**Design and Construction of HMA Overlays on Rubblized PCC Pavement**", National Asphalt Pavement Association.
- Ekdahl, P., "**A Sensitivity Test of Two Deterioration Modes for Flexible Pavements**", Ph.D Thesis, Department of Technology and Society, Lund Institute of Technology, Lund University, Sweden, 1999.



References

- Finn, F.N., and Monismith, C. L. NCHRP Synthesis of Highway Practice 116: **"Asphalt Overlay Design Procedures"**, TRB, National Research Council, Washington, D.C., pp. 66, 1984.

- Francken L., **"Laboratory Simulation and Modeling of Overlay Systems"**, Proc., 2nd International RILEM Conference-Reflective Cracking in Pavements, E & FN Spon, Liege, Belgium, pp. 75-99, 1993.

- Gaarkeuken G., Scarpas A. and de Boundt A. H., **"Causes and Consequences of Secondar Cracking"**, Road and Railway Research Laboratory, Delft University of Technology, Report 7-96-203-23, 1996.

- Griffith A. A., **"Philosophic Transactions of the Royal Society"**, A221, 1920.

- Gulden, W., and Brown, D., **"Treatments for Reduction of Reflective Cracking of Asphalt Overlays on Jointed-Concrete Pavements in Georgia"**, In Transportation Research Record 1007, TRB, National Research Council, Washington, D.C., pp. 26-36, 1985.

- Gurjar, A.H., Tang, T. and Zollinger, D. G., **"Evaluation of Joint Sealants of Concrete Pavements"**, Report No. 187-27. Texas Transportation Institute, College Station, Texas, 1997.



References

- Hertzberg, R., "**Deformation and Fracture Mechanics of Engineering Materials**", John Wiley and Sons, New York, 1996.
- Heukelom, W., "**Observation of the Rheology and Fracture of Bitumens and Asphalt Mixes**", Proceedings Association of Asphalt Paving Technologists, Vol. 35, pp. 358, 1966.
- Jacobs M. M. J., Hopman P. C. and Molenaar A. A. A., "**Application of Fracture Mechanics Principles to Analyze Cracking in Asphalt Concrete**", Proc., Annual Meeting of the Association of Asphalt Paving Technologists, Vol. 65, Baltimore, MD, pp. 1-39, 1996.
- Kanninen M. F. and Popelar C. H., "**Advanced Fracture Mechanics**", The oxford University Press, New York, 1985.
- Kim K. W. and El Hussein H. M., "**Effect of Differential Thermal Construction on Fracture Toughness of Asphalt Materials at Low Temperature**", Proceeding Association of Asphalt Paving Technologists, pp. 474, 1995.
- Lee N. K., Morrison G. R. and Hesp S. A. M., "**Low-Temperature Fracture of polyethylene Modified Asphalt Binder and Asphalt Concrete Mixes**", Proceeding of the Association of Asphalt Paving Technologists, Vol. 64, pp. 534, 1995.



References

- Lytton, R.L., "Use of Geotextiles for Reinforcement and Strain Relief in Asphaltic Concrete. Geotextiles and Geomembranes", Vol. 8, pp. 217-237, 1989.
- Lytton, R.L., Uzan, J., Fernando, E. G., Roque, R., Hiltunen, D., and Stoffels, S. M., "Development and Validation of Performance Prediction Models and Specifications for Asphalt Binders and Paving Mixes", Report No. SHRP-A-357. Strategic Highway Research Program, National Research Council, Washington, D.C., 1993.
- Majidzadeh K., Kaufmann E. M. and Ramsamooj D. V., "Application of Fracture Mechanics in the Analysis of Pavement Fatigue", Proceeding of Association of Asphalt Pavement Technologists, Vol. 40, pp. 227-246, 1970.
- Majidzadeh K., Ramsamooj, D. V. and Fletcher T. A., "Analysis of Fatigue of Sand-Asphalt Mixtures", Proc., Annual Meeting of the Association of Asphalt Paving Technologists, Vol. 30, Baltimore, MD, pp. 1-39, 1969.
- Marchand J. P. and Goacolou H., "Cracking in Wearing Courses", Proceedings of the 5th International Conference on the Structural Design of Asphalt Pavements, Delft University of Technology, 1982.
- McCullough, B. F., Chiu Liu, Dossey, T. and Cho, Y., "Asphalt Overlay Design Method for Rigid Pavements Considering Rutting, Reflection



References

- Cracking, and Fatigue Cracking "**, Center for Transportation Research, The University of Texas, Report No. 987-9, 1998.
- McLaughlin, A.L., "**Reflection Cracking of Bituminous Overlays for Airport Pavements, A State of the Art**" Report No. FAA-RD-79-57. Federal Aviation Administration, 1979.
- Mohammad L. N. and Paul, H. R., "**Evaluation of Indirect Tensile Test for Determining Structural Properties of Asphalt Mix**", In Transportation Research Record 1417, TRB, National Research Council, Washington, D. C., pp.58-63, 1993.
- Molenaar A. A. A., "**Effect of Modifications, Membrane Interlayers and Reinforcements on the Prevention of Reflection Cracking of Asphalt Overlays**", RILEM/CEP International Conference on Reflection Cracking in Pavements, University of Liege, Belgium, pp. 225, 1989.
- Neville, A. M., "**Properties of Concrete**", 3rd edition, Pitman, 1981.
- Paris, P. C. and Erdogan, E., "**A Critical Analysis of Crack Propagation Law**", Journal of Basic Engineering , Transaction of the American Society of Mechanical Engineering, Series D., Vol. 85, pp. 528-883, 1963.



References

- Pierce L. M., Jackson N. C. and Mahoney J. P., "**Development and Implementation of a Mechanistic, Empirically-Based Overlay Design Procedure for Flexible Pavements**", Transportation Research Record 1388, Transportation Research Board, Washington, D. C., pp. 120-129, 1993.
- Predoehl, N.H. , "**Use of Paving Fabric Test Installations in California**", Final Report. California Department of Transportation, Translab, 1989.
- Puzinauskas V. P., "**Properties of Asphalt Cement**", Research Report No. 80-2, Asphalt Institute, College Park, 1980.
- Ramsamooj D. V., "**Prediction of Reflection Cracking in Pavement Overlays**", HRR, No. 434, pp. 34, 1973.
- Read J. M., "**New Method for measuring Crack Propagation in Asphalts**", International Journal of Pavement Engineering, Vol. I, No. 1, pp. 15-34, 2000.
- Roberts, F.L., Kandhal, P. S., Brown, E. R., Lee, D. Y., and Kennedy, T. W., "**Hot Mix Asphalt Materials, Mixture Design and Construction**", NAPA Research and Education Foundation, Lanham, Maryland, 1996.
- RTAC, "**Transportation in Canada, Report No. 92**", Roads and Transportation Association of Canada, Pavement Committee, Transportation Association of Canada, Ottawa, 1972.



References

- Schapery R. A., "**Models for Damage Growth and Fracture in Nonlinear Viscoelastic Particular Composites**", Proc., 9th US Congress of Applied Mechanics, American Society of Mechanical Engineering, Book No. H00228, 1982.
- Shackelford, J.F, "**Material Science for Engineers**", 3rd Ed., Macmillan Publishing Company, New York, New York, pp. 355-357, 1992.
- Sherman, G. NCHRP Synthesis of Highway Practice 92: "**Minimizing Reflection Cracking of Pavement Overlays**", TRB, National Research Council, Washington, D.C., pp. 83, 1982.
- SORB, State Organization of Road and Bridge, 1982.
- Sulaiman S.J and Stock A. F., "**The Use of Fracture Mechanics for the Evolution of asphalt Mixes**", Proceeding of the Association of Asphalt Paving Technologists, pp. 500, 1995.
- Trevino, M., Dossey, T., McCullough and Yildirim, Y., "**Applicability of AC Overlays on Continuously Reinforced Concrete Pavement**", Center for Transportation Research, Report No. 0-4398-1, 2004.
- Uzan J., "**Evaluation of Fatigue Cracking**", Transportation Research Record 1570, Transportation Research Board, Washington, D. C., pp. 89-95, 1997.



References

- Vanelstraete A., Leonard, D. and Veys J., "**Structural Design of Roads With Steel Reinforcing Nettings**", Proc., 4th International RILEM Conference- Reflective Cracking in Pavements, E & FN Spon, Ontario, Canada, pp. 56-67, 2000.
- Zhou F. and Sun L., "**Reflection Cracking in Asphalt Overlay on Existing PCC**", Proceedings of the 9th International Conference on the Asphalt Pavements, Copenhagen, 2002.
- Zhou, F. and Scullion, "**Overlay Tester: a Rapid Performance Related Crack Resistance Test**", Texas Department of Transportation and the Federal Highway Administration, Report No. 0-446721, pp. 1-15, 2005.



Appendix A

APPENDIX OVERLAY TESTING PROTOCOL

1. Scope

- 1.1 This test method covers procedures for preparing and testing asphalt concrete mixtures to determine the reflection cracking resistance over a range of temperatures.
- 1.2 This test estimates the reflection cracking life based on the stress induced by the thermal movement at the bottom of the layer. Shear stress induced by the traffic load is not addressed in this test.
- 1.3 This standard is applicable to laboratory prepared specimens of mixtures and/or field cores with nominal maximum size aggregate less than or equal to 19.0 mm (0.75 in).
- 1.4 This standard may involve hazardous material, operations, and equipment. This standard does not purport to address all safety problems associated with its use. It is the responsibility of the user of this procedure to establish appropriate safety and health practices and to determine the applicability of regulatory limitations prior to use.

2. Referenced Documents

- 2.1 Texas Department of Transportation (TxDOT) Test Methods:
 - 2.1.1 Tex-241-F Superpave Gyrotory Compacting of Test Specimens of Bituminous Mixtures.
 - 2.1.2 Tex-207-F Determining Density of Compacted Bituminous Mixtures.
 - 2.1.3 Tex-227-F Theoretical Maximum Specific Gravity of Bituminous Mixtures.

3. Definitions

- 3.1 *Reflection Cracking Life* – N_{RCL} , the number of cycles needed to propagate cracking completely through a specimen under defined test condition.

4. Summary of Method

- 4.1 The repeated loading is applied until failure occurs at a loading rate of one cycle per 10 seconds using a cyclic triangular waveform with constant magnitude of 0.63 mm (0.025 in). The opening displacement and applied stress are measured and used to determine the reflection cracking life of asphalt mixture.
- 4.2 [Figure 14](#) shows the TTI overlay tester equipment. A specimen glued to the test plates is illustrated in [Figure 15](#). [Figure 16](#) shows a schematic of the test sequence.

Appendix A

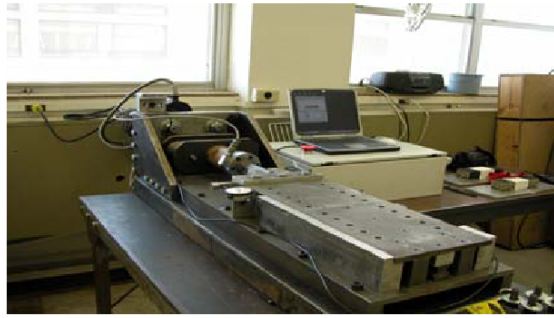
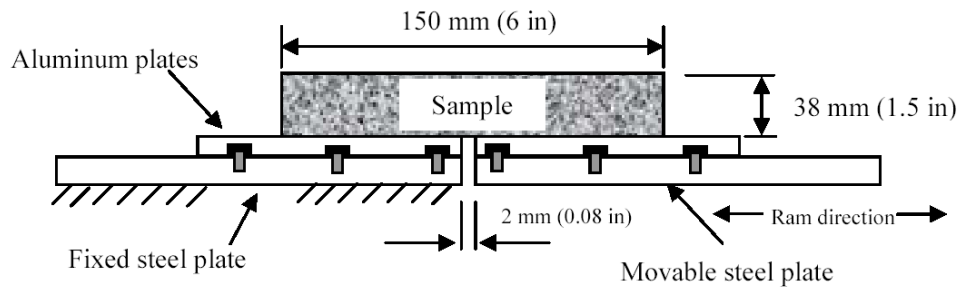


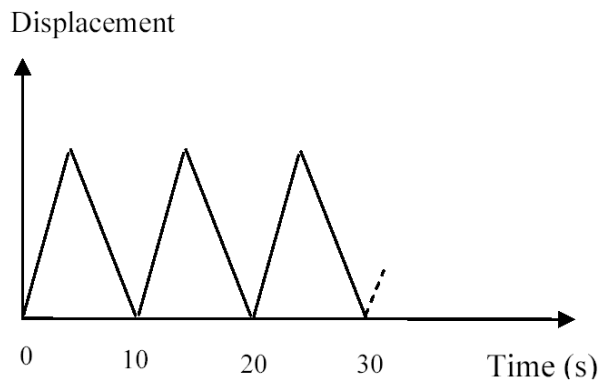
Figure 14. TTI Overlay Tester Equipment.



Figure 15. Test Specimen Glued to Plates.



(a) Concept of overlay tester



(b) Schematic of test sequence

Figure 16. Overlay Tester Procedure.

Appendix A

5. Significance and Use

- 5.1 Current TxDOT asphalt mixture design procedures do not consider the reflection cracking resistance of asphalt mixtures. In this test, the reflection cracking resistance of binder type and content, and aggregate can be measured.
- 5.2 The overlay tester simulates the performance of asphalt layers placed directly on top of concrete or cracked flexible pavements.
- 5.3 The reflection cracking life measured over a range of temperatures is an important design property. The results of this test can assist in binder type selection and overall mixture design.

6. Apparatus

- 6.1 *Overlay Tester System* — An overlay tester system consisting of a testing machine and measuring system plus environmental chamber if cold weather performance is required.
 - 6.1.1 *Testing Machine* — A mechanical testing machine driven by an electric motor through a gear box capable of producing a displacement controlled triangular waveform loading. The testing machine should have a capability of applying load over a range of loading periods from 2 to 10 hours and load levels up to 22.24 kN (5000 lb).
 - 6.1.2 *Environmental Chamber* (if required) — A chamber for controlling the test specimen at the desired temperature. The environmental chamber shall be capable of controlling the temperature of the specimen over a temperature range from 0 to 25 °C (32 to 77 °F) with an accuracy of ± 0.5 °C (1 °F). The chamber shall be large enough to accommodate the test specimen glued to plates and a dummy specimen with a thermocouple mounted at the center for temperature verification.
 - 6.1.3 *Measurement System* — The system shall be fully computer controlled; capable of measuring and recording the time history of the applied load plus the horizontal displacements. The system shall be capable of measuring the period of the applied load and resulting deformations with a resolution of 0.5 percent.
 - 6.1.4 *Plates* — Plates with a dimension of 300 mm (12 in) long by 150 mm (6 in) wide by 13 mm (0.5 in) high are required to glue the specimen on it. Grooves are cut in the plates at regular intervals as shown in [Figure 15](#). Generally, these plates should be made of hardened or plated steel, or anodized high-strength aluminum. Softer materials will require more frequent replacement. Materials that have linear elastic modulus properties and hardness properties lower than that of 6061-T6 aluminum shall not be used.

Appendix A

- 6.2 *Superpave Gyrotory Compactor* — A gyrotory compactor and associated equipment for preparing laboratory specimens in accordance with Tex-241-F is required.
- 6.3 *Saw* — A machine for sawing test specimens to the appropriate height and width is required. The saw shall have a water cooled diamond cutting edge and shall be capable of cutting specimens to the prescribed dimensions without excessive heating or shock to the specimen.

Note 1 — A diamond saw greatly facilitates the preparation of test specimens with smooth, parallel ends. Both single and double-bladed diamond saws should have feed mechanisms and speed controls of sufficient precision. Adequate blade stiffness is also important to control flexing of the blade during thin cuts.

7. Hazards

Observe standard laboratory safety precautions when preparing and testing HMA specimens.

8. Testing Equipment Calibration

- 8.1 The testing system shall be calibrated prior to initial use and at least once a year thereafter or per manufacturer requirements.
- 8.1.1 Verify the capability of the environmental chamber to maintain the required temperature within the accuracy specified.
- 8.1.2 Verify the calibration of all measurement components (such as load cell and specimen deformation measurement device) of the testing system.
- 8.2 If any of the verifications yield data that does not comply with the accuracy specified, correct the problem prior to proceeding with testing.

9. Test Specimens

- 9.1 *Size* — Overlay tester shall be performed on 150 mm (6 in) long by 76 mm (3 in) wide by 38 mm (1.5 in) high specimens sawed from gyrotory compacted mixtures or field cores.
- 9.2 *Gyrotory Specimens* — Prepare 150 mm (6 in) diameter by 57 mm (2.25 in) high specimens to the required air void content in accordance with Tex-241-F.

Note 2 — Testing should be performed on test specimens 38 mm (1.5 in) high meeting specific air void tolerances. The air void content of gyrotory specimens with 57 mm (2.25 in) high and 150 mm (6 in) diameter required to obtain a specified test specimen air void content must be determined by trial and error. Generally, the test specimen air void content is 1.5 to 2.5 percent lower than the air void content of the gyrotory specimen when the test specimen is removed from the middle of a 150 mm (6 in) diameter specimen.

Appendix A

Note 3 — Currently, it is recommended that laboratory prepared samples be molded to 7 percent air void content. This will better simulate the field condition. This will be upgraded as more results become available.

- 9.3 *Sawing* — The specimens are first cut to be 38 mm (1.5 in) high using the double-blade (or single-blade) saw. Then trim off 38 mm (1.5 in) from each side of the specimen. This is shown in Figure 17.

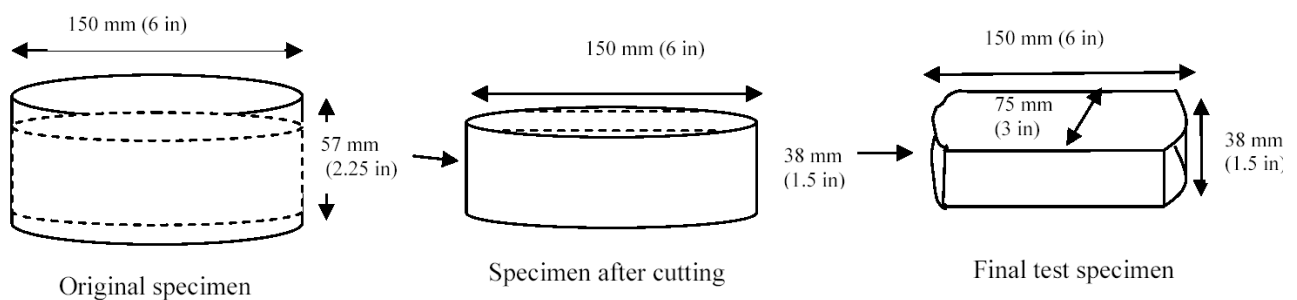


Figure 17. Process of Sawing Specimen.

- 9.4 *Air Void Content* — Determine the air void content of the final test specimen in accordance with Tex-207-F. Reject specimens with air voids that differ by more than 0.5 percent from the target air voids.

Note 4 — Considerable time can be saved if the cored test specimens were treated as wet, and the weights in water and saturated surface dry were measured immediately or within a short time period after sawing. The test specimens can then be left to dry overnight, the dry weight can be measured the next day, and then they can be immediately prepared for testing.

- 9.5 *Replicates* — The number of test specimens required depends on the desired accuracy of the overlay tester results. Three replicates are recommended for each mixture.
- 9.6 *Specimen Storage* — Wrap completed specimens in polyethylene and store in an environmentally protected storage area at temperatures between 5 and 25 °C (41 and 77 °F).

Note 5 — To eliminate the effects of aging on test results, it is recommended that specimens be stored no more than two weeks prior to testing.

10. Gluing the Specimen to the Plates

- 10.1 A cut specimen is epoxied to the horizontal surface plates with half the length of the beam resting on each plate. Then, put a 4.5 kg (10 lb) or more metal block on the top of the specimen to make sure the specimen sticks to the plates.

Appendix A

Note 6 — Devcon™ two tone 30-Minute Plastic Steel Epoxy Cement is satisfactory for tests conducted at 0 to 25 °C (32 to 77 °F).

10.2 The glued specimen needs to cure at room temperature, 25 °C (77 °F), for 4 hours in order to let the glue gain enough strength.

11. Test Procedure

11.1 The recommended test protocol for the overlay tester for use in asphalt mixture design consists of testing the asphalt mixture at a specified temperature (e.g., 25 °C [77 °F]) and opening displacement of 0.63 mm (0.025 in).

Note 7 — For the testing temperature, it is recommended that overlay tester be conducted at room temperature. In the future, the effective pavement temperature, T_{eff} , (a single test temperature at which reflection cracking would occur equivalent to that measured by considering each season separately throughout the year) will be determined for overlay tester.

Note 8 — The opening displacement of 0.63 mm (0.025 in) is determined based on the following assumptions and calculations:

- Daily temperature variation (Δt): 30 °F
- Slab length (l): 15 ft
- Coefficient of thermal expansion of PCC (α_t):

For PCC with gravel: 6×10^{-6} in./in./°F

For PCC with limestone: 3.5×10^{-6} in./in./°F

Since displacement = $\Delta t * l * \alpha_t$,

displacement for PCC with gravel is 0.0324 in ($=30 * 15 * 6 * 10^{-6}$)

displacement for PCC with limestone is 0.0189 in ($=30 * 15 * 3.5 * 10^{-6}$)

The average displacement is approximately 0.63 mm (0.025 in), which is recommended for overlay tester.

11.2 Place the test specimen glued to the plates in the environmental chamber and allow it to equilibrate to the specified testing temperature. A dummy specimen with a temperature sensor mounted at the center can be monitored to determine when the specimen reaches the specified test temperature. Currently, it is recommended that the overlay tester be conducted at room temperature (25 °C [77 °F]).

11.3 Fix the plates with glued specimen to the overlay tester using bolts to make sure that the plates move with the overlay tester in a unit.

Appendix A

- 11.4 The repeated loading is applied until failure occurs at a loading rate of one cycle per 10 seconds using a cyclic triangular waveform with constant magnitude of 0.63 mm (0.025 in) as shown in [Figure 16](#).

12. Calculations

- 12.1 Determine the air voids for each specimen.
- 12.2 Determine the reflection cracking life of each specimen.

Note 9 — An Excel Macro is under development to automatically determine the reflection cracking life, and will be delivered to TxDOT.

13. Report

- 13.1 Report all specimen information including mix identification, storage conditions, dates of manufacturing and testing, volumetric properties, test temperature, opening displacement, and reflection cracking life.

Symbols and Abbreviations

- A : Fracture Parameters of The Material.
- a : Slope of The Fatigue Curve.
- AC : Asphalt Content (%).
- ACC: Asphalt cement concrete.
- ASTM: American Society for Testing and Materials.
- AV : Air Voids (%).
- B : The Depth of The Beam.
- BRCC :Belgian Road Research Center.
- C : Constant of The Fatigue Line.
- c : Crack Length.
- c: Crack Length.
- COTE: Coefficient of Thermal Expansion.
- d: Crack Depth.
- E : Resilient Modulus of The Mixture.
- $f(c/d)$: Dimensionless Parameter That Depends on The Length (c) and
- HMA: Hot Mix Asphalt.
- K : Stress Intensity Factor.
- K_{IC} : Stress Intensity Factor at Fracture Toughness.
- m : Slope of The Log Creep Compliance Versus Log Time Curve.
- n : Fracture Parameters of The Material.
- N : Number of Loading Cycles.
- N_i : Number of Cycles Before Crack Initiation.
- N_f :The Number of Load Cycles Needed to Propagate a Crack Through The Asphalt Overlay Thickness.
- PCC: Portland Cement Concrete.
- P_f : The Failure Load.
- POT: Pavement Overlay Tester.
- r: Distance From The Crack Tip to The Analyzed Element.
- RTAC: Roads and Transportation Association of Canada.
- S : The Span Fixed at 100 mm.
- SAMI: Stress Absorbing Membrane Interlayer .
- SMA: Stone Mastic Asphalt.
- SORB: State Organization of Road and Bridge.
- w : The Width of The Beam.
- y: Dimensionless Parameter That Depends on Both Specimen and Crack Geometry.
- ϵ_{zx} : Shear Strains 10 mm Above The Existing Crack.
- ϵ : Critical Strain.
- σ : Nominal Stress.
- σ_f : The Failure Stress Within The Body Far Away From The Crack.